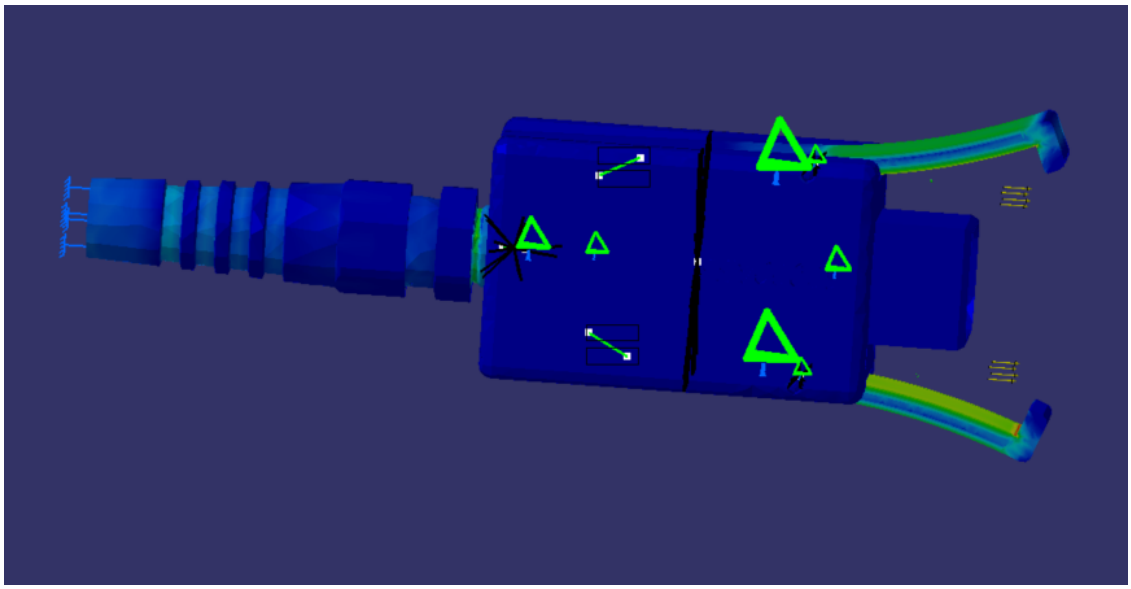

Investigative Study of 3D Printed Connectors in Volvo Trucks production

A Comparison of Methods and Materials

Master's thesis in Applied Mechanics

LINNEA PIHL

DEPARTMENT OF MECHANICS AND MARITIME SCIENCES

CHALMERS UNIVERSITY OF TECHNOLOGY
Gothenburg, Sweden 2025
www.chalmers.se

Master's thesis 2025

Investigative Study of 3D Printed Connectors in Volvo Trucks production

A Comparison of Methods and Materials

LINNEA PIHL

CHALMERS
UNIVERSITY OF TECHNOLOGY

Department of Mechanics and Maritime sciences
Chalmers University of Technology
Gothenburg, Sweden 2025

Investigative Study of 3D Printed Connectors in Volvo Trucks production
A Comparison of Methods and Materials
LINNEA PIHL

Supervisor: Richard Ernfjäll, Volvo AB
Examiner: Ragnar Larsson, Industrial and Materials Science

Master's Thesis 2025
Department of Mechanics and Maritime Sciences
Chalmers University of Technology
SE-412 96 Gothenburg
Telephone +46 31 772 1000

Cover: Finite Element simulation of connector analyzed in this thesis work.

Typeset in LaTeX
Printed by Chalmers Reproservice
Gothenburg, Sweden 2025

Investigative Study of 3D Printed Connectors in Volvo Trucks production
A Comparison of Methods and Materials
LINNEA PIHL
Department of Mechanics and Maritime Sciences
Chalmers University of Technology

Abstract

All vehicles that are produced today by Volvo are provided with software that controls the vehicle. In Volvo Trucks production facilities, connectors are used to download software to the vehicle by using connectors. This master thesis is carried out together with Volvo group AB and aims to conduct an investigative study to evaluate whether the connectors used could be 3D printed, used as spare parts and used in Volvo's production. To analyze whether it is feasible to use a 3D printed connector in production, a material study was carried out, and a finite element analysis was performed on both existing and 3D printed connectors. The material study included tensile testing of the following polymer materials: Sustarine, PLA, PLA-CF, PETG, PETG-CF, TPU, and PATH-CF. In addition to tensile testing, the 3D printed test samples were also observed for surface quality and dimensional accuracy.

From the material study, it was found that the PLA, PLA-CF, PETG and PETG-CF materials were suitable to print connectors in. PATH-CF was excluded due to challenges in achieving acceptable print settings and the poor surface quality it produced, and TPU was excluded due to issues such as deformation in corners and holes and insufficient layer bonding. From the finite element analysis it could be seen that all materials except TPU could be suitable to print the connectors. The TPU material was unsuitable because it was the only material in which the von Mises stress exceeded the material's yield strength. The results indicate that it would be possible to use a 3D printed connector as a spare part. To be able to know if a 3D printed connector could have completely replaced a purchased connector, more studies would have needed to be done, such as fatigue analysis and material wear.

Keywords: 3D printing, Finite element analysis (FEA), PLA, PLA-CF, PETG, PETG-CF, TPU, PATH-CF

Acknowledgements

I would like to express my sincere gratitude to everyone who has supported and encouraged me throughout the course of this thesis work.

First and foremost, I would like to extend my heartfelt thanks to Volvo Group AB, the ESW Tools, Systems & Strategy Group and my industrial supervisor Richard Ernfjäll for their generous support, valuable insights, and continuous guidance during this project. Your expertise and feedback were instrumental in helping me navigate challenges and complete the work successfully.

I am also deeply grateful to my academic supervisor and examiner at Chalmers, Ragnar Larsson, for his academic guidence, constructive critique, and consistent support throughout the process. Your academic perspective helped me improve the quality of the thesis work.

Finally, I would like to thank my family for their encouragement and support, whose support has been truly invaluable throughout this process.

Linnea Pihl, Gothenburg, June 2025

List of Acronyms

Below is the list of acronyms that have been used throughout this thesis listed in :

ABS	Acrylonitrile Butadiene Styrene
AM	Additive manufacturing
DOF	Degrees of freedom
ECUs	Electric control units
FEA	Finite Element Analysis
FEM	Finite Element Method
G-code	Code generated by slicer
PLA	Polylactic Acid
PLA-CF	Carbon fiber reinforced PLA
PETG	Polyethylene Terephthalate Glycol
PETG-CF	Carbon fiber reinforced PETG
PATH-CF	Carbon fiber reinforced Nylon 12
TPU	Thermoplastic Polyurethane

Contents

List of Figures

List of Tables

1
Introduction

This chapter presents the background necessary to understand why the thesis is carried out. The chapter also presents the aim and limitations of the project, as well as the use of artificial intelligence.

1.1 Background

All vehicles produced today by Volvo trucks are provided with software that controls many of the different features and functions in the vehicle. For example, a window goes down when pressing a button, or a warning goes off if one is driving without the seatbelt. These different functions are managed by small computers called electronic control units (ECUs), which are placed at several different places on the truck. During production, connectors are used to connect to the different ECUs, to download softwareto the vehicle. This is done in multiple places on the production line and in different parts of the vehicle. These different vehicle parts need different types of connectors. The connectors are designed and manufactured by other companies and then purchased by Volvo. Volvo decides on what functions and properties that are needed, and the company manufactures a prototype that Volvo evaluates.

Figure 1.1: Connector studied in this thesis project.

It is an iterative process in which Volvo and the company send the prototype back and forth until Volvo is satisfied with the product. The connector that will be studied in this thesis, see Figure 1.1, is used at a sub-assemblage station for engine assembly. The connector is fixed at a software download station and the vehicle is attached to the production line that constantly moves forward.

1.2 Aim

The purpose of this thesis is to conduct an investigative study to evaluate whether it is possible to 3D print connectors in Volvo trucks production facilities that can be used in the factory as spare parts or as replacement of existing connectors, and if it is feasible to use 3D printed connectors during prototype testing and validation. Investigate whether FEM analysis can be used reliably on 3D printed materials and to identify possible error sources and limitations using 3D printed connectors. The aim of the thesis is to support the company in the decision-making process around 3D printing as a manufacturing method for spare parts or parts used in production, which can contribute to a more efficient development process, reduced costs, and improved environmental impact.

1.3 Limitations

The following limitations are set on this project:

1. The digital model will be simplified to contain no screws, springs, or pins.
2. The thesis will not include lateral loads.
3. The materials that the study will examine are PLA, PLA-CF, PETG, PETG-CF, TPU95A, PATH-CF
4. There will be no comparison between different 3D printers.
5. There will be no comparison between different infill percentages or infill structures.
6. The study is limited to being conducted for 20 weeks.

1.4 Problem formulation

To clarify and simplify the main problem, the thesis is divided into different problem areas. The problem areas were then divided into different sub-objectives that should be met in order to carry out the work.

1. Examine which material is suitable for 3D printed connectors through tensile testing, property testing, ease of printing, and physical results of printing.
2. Investigate which parts of the connector that is suitable for 3D printing.
3. What type of load case should be investigated?
4. Investigate 3D printed connectors during the selected load case by performing finite element analysis and physical testing.
5. Examine if the finite element analysis matches the physical testing of the 3D printed connectors in the different materials.

6. Compare the results between machined and 3D printed connectors based on the stresses that occur during the selected loadcase.
7. How does the chosen material and 3D printing as a manufacturing method affect the environment compared to the machined connector?

1.5 Use of artificial intelligence

When it comes to using artificial intelligence (AI) tools, it is important to be aware of the risks involved. According to Chalmers guidelines, the student must use AI in a responsible and transparent manner [7]. The student must assume full responsibility and be able to justify the content and choices made, as well as clearly show what and how AI has been used. In this work, AI has not been used to make decisions, develop methods and results, or generate text. AI has been used as a tool to troubleshoot the 3D printer, find where certain specific settings are in the slicer software, and provide suggestions for improvements and wording in the report.

2
Theory

In this chapter, all relevant theory will be presented. This includes the theory of the selected connector, the selected load case, 3D printing, finite element analysis, and materials.

2.1 Selected connector and load case

As described in Background 1.1, the connector is used in the production of Volvo Trucks. The connector is fixed at a station where an operator connects it to the sub-module that will be programmed with software. The part of the vehicle that will be programmed is constantly moving on the production line. The case that will be studied in this project is an event in which the operator forgets to disconnect the connector from the adapter in time, and the sub-assembly continues to move while still attached to the connector. The connector will then be exposed to a force and the case is to investigate what force the current machined connectors can withstand and what force a 3D printed connector printed in the factory could withstand.

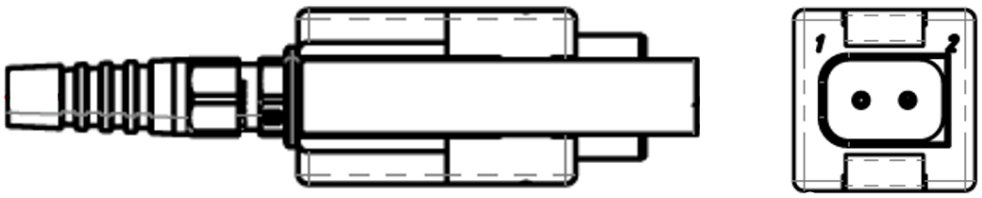

Figure 2.1: Drawing of the connector provided by Volvo Trucks.

The connector consists of two main parts that are screwed together with metal screws, two clamps that are attached via a metal shaft, and a cable gland that stabilizes the cord. In the connector, there are also two springs per clamp. A

drawing of the connector can be seen in Figure 2.1 and how the different parts are put together can be seen in Figure 2.2.

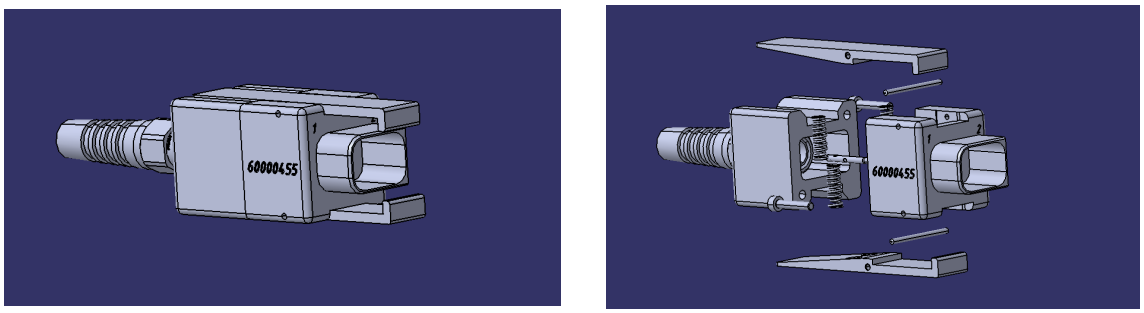

(a) (b)

Figure 2.2: Catia model of how the parts of the connector fit together.

2.2 Finite Element Analysis

The Finite element method (FEM) is a numerical method used to solve partial differential equations by dividing a complex geometry into smaller simpler parts called finite elements. Instead of solving the differential equation for the entire domain, FEM approximates the solution within each finite element. This makes it possible to approximate solutions to problems that would be difficult to analyze analytically. [2]. The points where elements are connected to each other are called nodes, and each node has an associated set of degrees of freedom (DOF). Using the DOFs of the nodes together with predefined equations, the behavior of each element can be determined based on known material properties. This process is performed on all elements, resulting in an approximate solution for the entire domain.

Finite element analysis (FEA) is the practical application of FEM. The first step to performing an FEA analysis is mesh generation of the object which will be analyzed. When a mesh is generated, the geometry of the object is divided into finite elements. The mesh size (size of the elements) will determine the accuracy of the solution. A main rule is that a finer mesh with smaller elements gives a more exact solution, but also requires more computing resources and takes longer time to simulate. To avoid performing simulations that take an unnecessary long time, it is common to perform a mesh sensitivity study to determine when convergence of the results is reached. A mesh sensitivity study aims to establish the optimal mesh configuration. This is done by systematically changing the mesh size and observing the solution. When the solution result does not change more than the intended accuracy, the solution can be considered to be converged. If the geometry which will be simulated is complex or has, for example, a small radius, a local mesh size can be applied, which means that meshing is only refined where necessary.

The chosen material is defined in the FEA software. When a polymeric material is modeled, properties such as density and elasticity are needed. These properties

include Young's modulus(E), Poisson's ratio (ν), yield stresses (σ_y) and density (ρ). These properties can be obtained by either using existing data sheets or analyzing stress-strain curves extracted from material testing data.

2.3 3D Printing

Additive manufacturing (AM) is a technology that is capable of creating physical 3D objects from a digital model. An AM method is 3D printing, where the digital model is broken down into 2D cross sections, called layers, by using a program called a slicer. The slicer software then generates a G-code that can be sent to the 3D printer. Using the G-code, the 3D printer can create the physical object by a layer-by-layer sequence. The 3D printer melts the material and extrudes the melted material through a nozzle in the layers generated by the slicer software. The layers solidifies and combines to create the 3D object. The AM technology was initially developed for use in polymeric materials, but has since evolved to introduce other materials such as composites and metals [1].

When the digital 3D model has been imported into the slicer software, many different settings can be changed to achieve the best possible result. Some important parameters which should be taken into account are the nozzle temperature, the builder plate temperature, volumetric speed limitation, fill percentage, infill structure, support structure, and orientation of the object that will be printed. The temperature settings of the nozzle and the builder plate depend on the material chosen. The nozzle temperature is especially important since it directly affects the 3D printed result. A too high nozzle temperature heats the material too much, which can lead to over extrusion, which in turn can cause surface defects and weakened prints. On the other hand, too low nozzle temperature will not heat the material sufficiently and this can cause the layers to not adhere to each other properly [10]. This and a slower flow rate from the material not being melted enough can lead to print failures. The bed temperature is important to ensure that the first layer adheres to the printing bed, if the first layer does not adhise it will be printing failure [10]. The volymetric speed limitation settings refer to how much plastic the 3D printer will extrude per second. This is a crucial factor that decides how fast the printer can print while keeping the quality of the prints. The speed at which a material can be extruded without affecting the quality of the print varies between different materials, and the speed is often specified by the manufacturer.

Normally, when an object is 3D printed, it is not printed as a solid object but as an object with an inner and outer shell that are filled with and infill structure. The percentage of fill refers to how much space between the inner and outer shell walls is filled with this fill structure. An 100% infill would mean that the object is solid and an 0% infill would mean that the object is printed as a shell. A low filling percentage entails that the object is printed quickly but that, on the other hand, gives lower stiffness and durability, while a high filling percentage makes the object stronger but takes more time to print and also requires more material. Infill settings

can also be changed to different types of infill structure.There is a possibility that the printed material does not have enough time to solidify properly when printing complex geometries or models with overhanging parts. Therefore, it is common for models to be printed with a support structure. A support structure can strengthen overhanging parts during printing and make sure that the material solidifies correctly. A support structure should be printed in such a way that it can be removed easily from the object after the object has been printed. The support structure is generated in the slicer program. It is important to choose the option, support from builder plate only, if all support structures are to be properly removed. This option ensures that the support structure will only be generated on the outside of the object and not inside the infill structure. It is beneficial to avoid support structure if possible, as it takes time to print and remove the material, and it costs money to print the extra material. If needed, the support structure can be printed in a different material from the main object, as long as the printer can handle more than one material at the time.

The orientation of the object can be changed to avoid using a support structure. By rotating the object in such a way that the structure supports itself, all supporting structures can be removed. Another thing to consider regarding orientation of the object is that 3D printed parts are stronger along the layers compared to across them[9]. Therefore, it is advantageous to position the object in such a way that it is printed with the layers in the correct direction for the finished object to be as strong as possible. The precision of holes and other details also varies depending on how the object is oriented. Holes, for example, have very good precision when printed laying down compared to when standing, as there is an overhang that can make the holes less precise, which is also something to consider when orienting the object.

2.4 Materials

In this Section different filament materials used for 3D printing and their properties will be discussed as well as material properties for the purchased connectors that are used in factories today.

2.4.1 PLA

Polylactic acid (PLA) is a biodegradable filament and is one of the most commonly used filaments since it is easy to use and has low printing temperatures. PLA is mainly used for prototypes and decoratives as it is stiff but relatively brittle and has low heat resistance[8]. PLA is also available in combination with carbon fiber, PLA-CF, which provides increased stiffness and strength. Carbon fiber reinforced plastic components are often used for functional prototypes and for applications that requires high mechanical loads[5]. However, with carbon-reinforced polymers, there are some challenges regarding recycling. If the material is recycled, it is difficult to separate carbon fibers from the polymer material[6]. If the fibers are successfully separated, there are still challenges, such as the difficulty of not damaging the fibers during the process, which is necessary for the fibers to retain their properties.The

material data for PLA and PLA-CF are provided by the manufacturer[8] and can be seen in Table 2.1.

Table 2.1: Material data for PLA and PLA-CF from the manufacturer.

Material	$E\ [MPa]$	$\rho[kg/m^3]$	$\sigma_y\ [MPa]$
PLA	2870	1240	58
PLA-CF	2960	1240	62

2.4.2 PETG

Polyethylene Terephthalate Glycol (PETG) is also one of the most commonly used materials used for 3D printing, mainly since the material has a great chemical resistance. PETG is a strong, durable and partially flexible plastic that combines the advantages of both PLA and ABS and, due to the properties of the material, it is suitable for technical applications[8]. PETG is also available as an alternative with elements of carbon fiber (PETG-CF), and, as previously mentioned, an addition of carbon fiber provides increased stiffness and strength. The material data provided by the manufacturer[8] can be seen in Table 2.2.

Table 2.2: Material data for PETG and PETG-CF from the manufacturer.

Material	$E\ [MPa]$	$\rho[kg/m^3]$	$\sigma_y\ [MPa]$
PETG	1651	1270	45
PETG-CF	5120	1320	52

2.4.3 TPU

Thermoplastic Polyurethane (TPU) is a versatile filament. It has high wear resistance, and since it is a ductile filament it is possible to print highly flexible parts. However, it requires a slower printing speed compared to most other filament materials[8]. No material data was presented by the manufacturer for TPU.

2.4.4 PATH-CF

PATH-CF is a carbon fiber-reinforced Nylon 12 filament. The material has properties such as being highly wear-resistant, chemically and UV resistant, and having good layer adhesion. The material is usually used for 3D-printing end-use parts. The carbon fibers make the material stiffer and less prone to shrinkage but not stiff enough to reduce the Nylon's extreme impact resistance. However, the material is more technical to print [8]. The material data provided by the manufacturer[8] can be seen in Table 2.3.

Table 2.3: Material data for PATH-CF from the manufacturer.

Material	$E\ [MPa]$	$\rho[kg/m^3]$	$\sigma_y\ [MPa]$
PATH-CF	1460	1200	58

2.4.5 Sustarine

Sustarine is the material of which today the connectors purchased are made. The material has high stiffness, high dimensional stability, and is electrically conductive. Material data is provided by the manufacturer [11], see Table 2.4.

Table 2.4: Material data for Sustarine from the manufacturer.

Material	E $[MPa]$	$\rho[kg/m^3]$	σ_y $[MPa]$
Sustarine	3700	1440	45

2.5 Sustainability

In this section, 3D printing as a manufacturing method will be compared to the method currently used for the connectors, which is mainly milling, from a sustainability perspective. One major difference between AM and traditional machining is material waste. In machining, complex geometries, such as connectors, often require substantial material removal. This results in significant material waste compared to 3D printing, which generates minimal waste, typically limited to initial priming and, if required, support structures. According to Faludi et al. (2015), who compared the environmental impact of 3D printing with a traditional computer numerical control milling machine through a life cycle analysis, the main impact of 3D printing is the use of electricity and for the machining, material waste, and cutting fluid, where the main impacts [3]. Faludi et al. mention that 3D printing had lower ecological impacts per produced part compared to machining. 3D printing also enables local production that reduces transportation-related emissions [4].

3
Methods

In this chapter, the different methods used in the project will be presented. This includes 3D printing, FEA, material choice, and physical testing.

3.1 Material investigation

To gain a better understanding of the printability and mechanical behavior of the materials, a brief material study was conducted. In order to be able to use the 3D printed connector as a spare part or replacement for an existing connector, the selected material needed to withstand equivalent mechanical loads without yielding. When used for prototype testing, the ability to give good surfaces and precise printing is more valuable. Additionally, it had to be a polymer compatible with the available 3D printer. To evaluate this, standardized test specimens were 3D printed to observe surface quality and dimensional accuracy. Tensile tests were also performed on the test specimens to obtain the material properties of the materials.

3.1.1 Poisson's ratio

There were no exact Poisson's ratio values provided from the manufacturer for any of the materials. Therefore, the values were approximated based on typical ranges for plastic materials found in engineering literature and databases such as MatWeb. Typical Poisson's ratio values for polymers are 0.33-0.4 [12][13][14] where 0.35 was estimated to be the most common value. An exception was made for TPU, which is a flexible material, and the value 0.45 was estimated.

3.1.2 3D printing test specimens

The 3D printer used for this project was Flashforge Guider 3 Ultra and it was used together with the Orca flashforge 1.3.1 slicer program and the Bambu lab X1C with the Bambu studio slicer. The geometry of the test specimens was created in Catia and followed the ISO 527 standard. The drawing and complete test specimen can be seen in Figure 3.2, Appendix .7, for bigger picture.

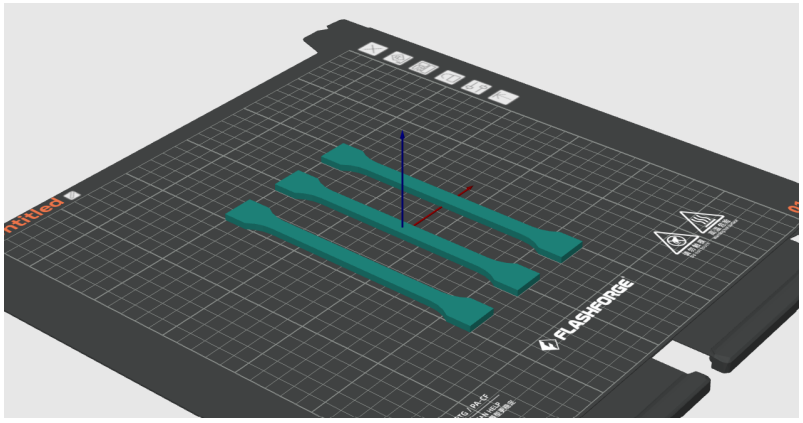

Figure 3.1: Test specimens in slicer program.

The test specimens were printed on the following materials: PLA, PLA-CF PETG, PETG-CF, TPU, and PATH-CF. For the orientation of the test specimens on the printer bed, see Figure 3.1. The 3D printers settings was changed in the slicer for each material to obtain best possible results. For more details on the settings, see Appendix .1

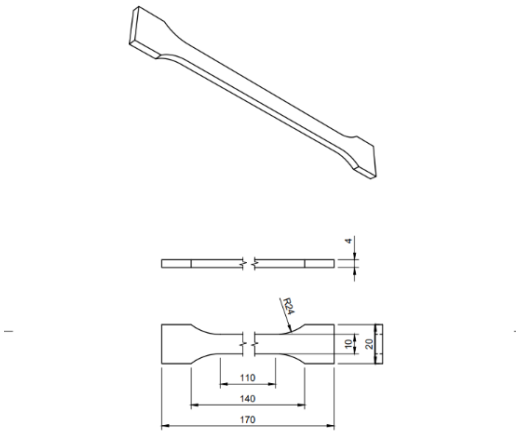

(a)

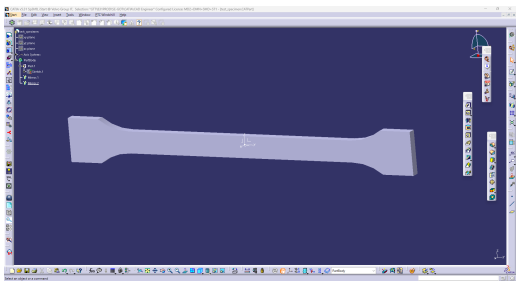

(b)

Figure 3.2: Drawing and complete test specimen in Catia V5.

3.1.3 Tensile testing on test specimens

When performing the tensile tests on the test specimens, the plastic tension option was used on the tensile testing machine. Other settings in the machine were:

1. Test speed 10mm/min
2. Prestress 0.2MPa
3. extensiometer max 3%
4. extensiometer measure 2%.

For a visual representation of the test setup, see Figure 3.3

Figure 3.3: Test setup for 3D printed test specimens.

3.1.4 3D printing connectors

The two parts of the connector housing were printed separately and the clams were printed together. The parts and their orientation on the printing bed can be seen in Figures 3.4, 3.5 and 3.6. The support structure was used when printing the second part of the connector housing and the option *support from builder plate only* was used.

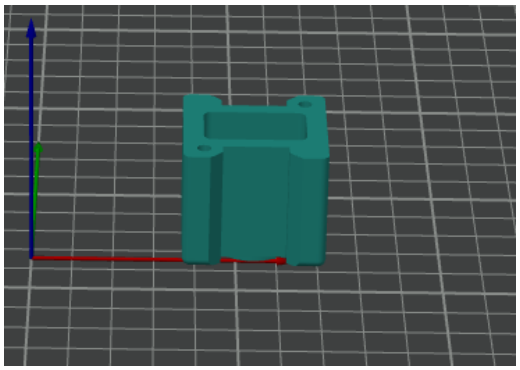

(a)

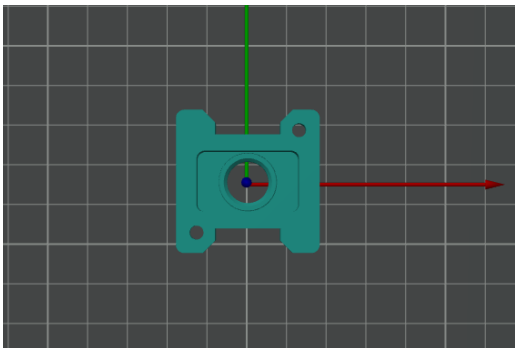

(b)

Figure 3.4: Part one of the connector housings orientation in slicer.

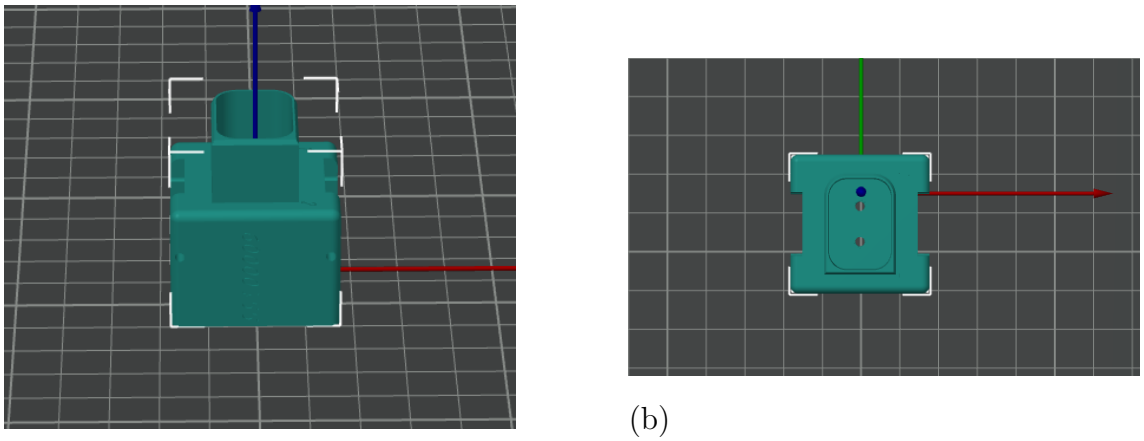

(a) (b)

Figure 3.5: Second part of the connector housings orientation in slicer.

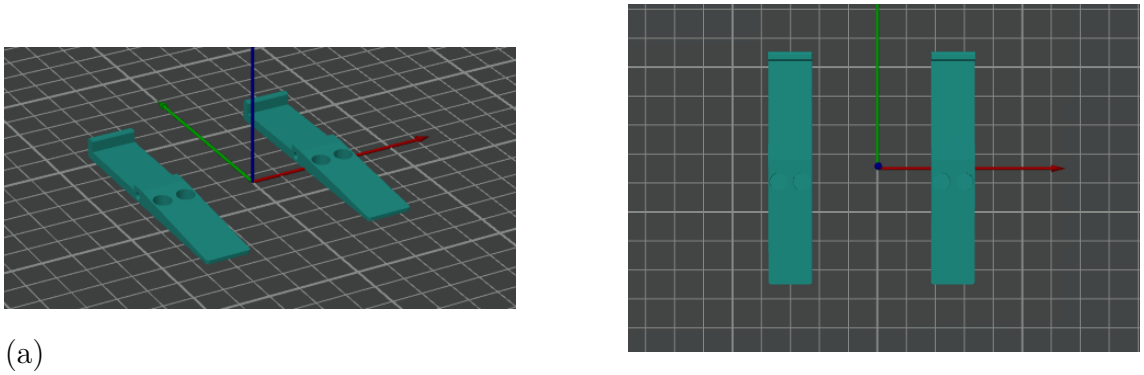

(a) (b)

Figure 3.6: Orientation of the clams in slicer.

3.2 Tensile test purchased connector

A tensile test was performed to determine the force the connector can withstand before being released from the adapter. When the force is known, it can be used in the FEA to see if the 3D printed connectors would be able to withstand the same force or if they would break. The following settings were used on the tensile testing machine during the test:

1. Type of test: tension-tension
2. sample length 55.0mm
3. sample width 35.0mm
4. sample thickness 35.0mm
5. sample weight 162.0g
6. test speed 30mm/min
7. contacts speed 10mm/min
8. return speed 300mm/min
9. stop load 95%

10. minimum travel 1mm
11. contact load $1N$
12. max test load $1000N$

To mimic the load case mentioned in Section 2.1, the connector was attached to the cable gland and connected to the adapter. The adapter was also attached to the machine through its cable gland. The setup can be seen in Figure 3.7.

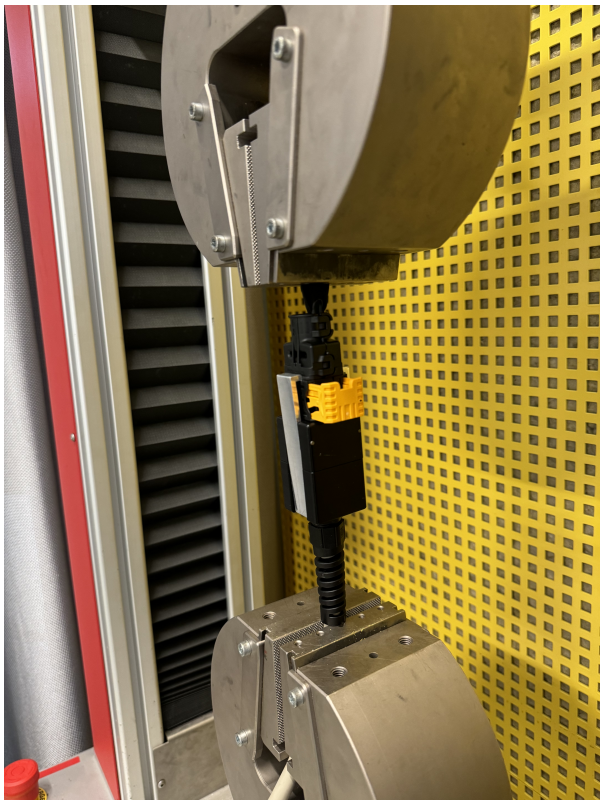

Figure 3.7: Tensile test setup of the purchased connector.

3.3 Finite Element Analysis

The goal of the FEA on the purchased connector is to find out where the stress concentrations occur and to see if the connector behaves as expected based on the physical test performed. The goal of FEA on the 3D printed connectors is to see if they would withstand the same force that was required for the purchased connector to release from the adapter without reaching the yield limit.

The assembly of the connector provided by the company was opened in the FEA program. To simplify the model, all screws, springs, and pins were removed from the assembly. The remaining components were the two main parts that make up the contact housing, two clamps with attachment shafts, and the cable gland. To mesh parts, the Advance surface mesher was used with parabolic elements and mesh size 8mm with an absolute sag of 0.8mm.
The material was then defined and applied to the parts. The material properties used

when simulating the purchased connector came from a material data sheet provided from the connector manufacturer, see Table 3.1. For the Poisson´s ratio, the value 0.35 and 0.45 was used according to Section 3.1.1. The material properties used when simulating the 3D printed connectors came from data sheets from the manufacturer, and for the materials which had missing data, parameters found from the physical material tensile tests were used. The material data used when simulating 3D printed connectors can be seen in Table 3.1.

Table 3.1: Material data used during FEA simulations.

Material	$E\ [MPa]$	$\rho[kg/m^3]$	$\sigma_y\ [MPa]$	$\nu\ [\ ]$
Sustarine	3700	1440	45	0.35
PLA	2870	1240	58	0.35
PLA-CF	2960	1240	62	0.35
PETG	1651	1270	45	0.35
PETG-CF	5120	1320	52	0.35
PATH-CF	1460	1200	58	0.35
TPU	62	1200	9.13	0.45

In order for the analysis tool to understand how the assembly is constrained, connections and boundary conditions were added. To mimic the steel screws that hold the two main parts of the contact housing together, a rigid connection is used, see Figure 3.8. The rigid body connection restricts the movement of the selected surfaces so that the relative positions of the points on the surfaces remain constant throughout the analysis, which means that the surfaces cannot be released from each other. The same type of rigid connection was used between the contact housing and the cable gland, see Figure 3.9. The shafts that attach the clamps to the connector housing were constrained using rigid connections between the outer surface of the shafts and the inner surface of the connector housing holes, see Figure 3.10. In the same way, the clamps were also connected to the shaft with a rigid connection, see Figure 3.11. To allow the clamps to rotate around the shaft, the degree of freedom that rotates around the shaft was released. To ensure that the clamps and the contact housing cannot move through each other, a contact connection was also needed between the underside of the clamp and the outside of the contact housing, see Figure 3.12.

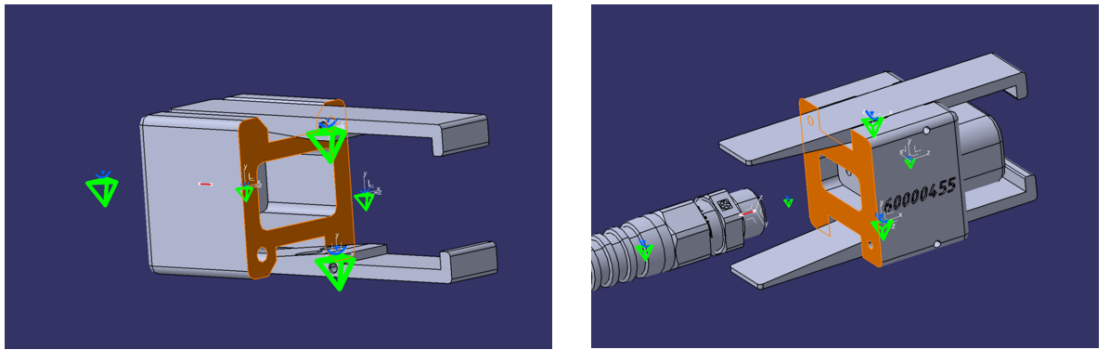

Figure 3.8: Rigid connection between the first and second parts of the connector housing.

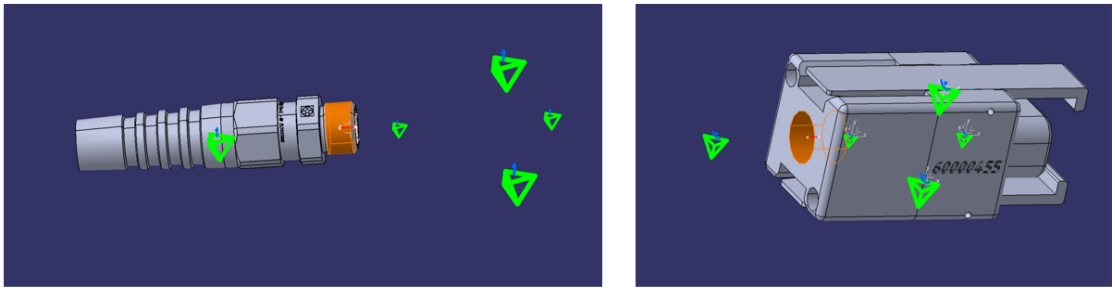

Figure 3.9: Rigid connection between cable glamp and the back part of the connector housing.

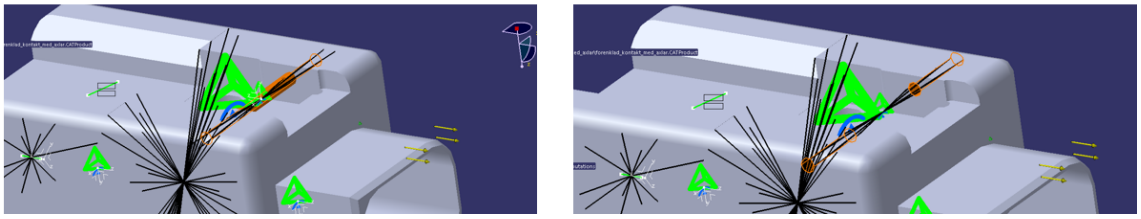

Figure 3.10: Rigid connection between the shaft and connector housing.

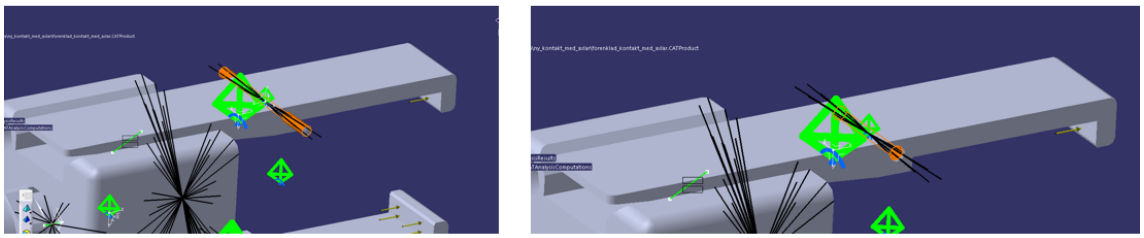

Figure 3.11: Rigid connection between the shaft and clams.

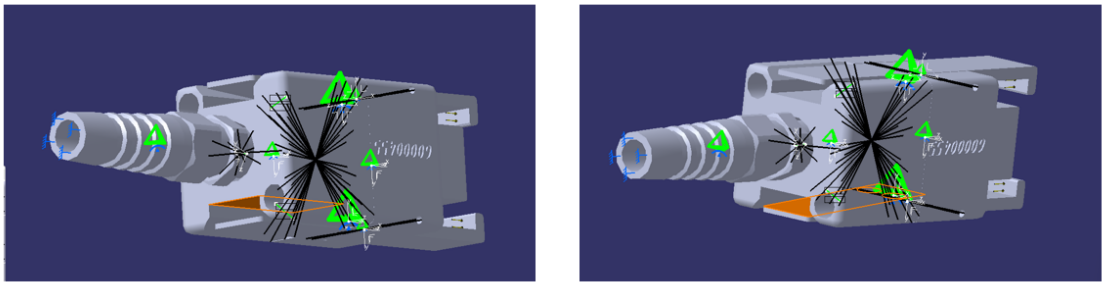

Figure 3.12: Contact connection between the connector housing and clams.

Next, the boundary conditions were added. To resemble the selected load case, the sub-assembly was clamped at the end of the cable gland. The boundary condition can be seen in Figure 3.13. The second boundary condition was a distributed force that was added to the interior of the clams. The magnitude of the force was the maximum force that was found during the physical tensile test performed on the connector, and the force had the same direction as the local x-axis of the clams, see Figure 3.14.

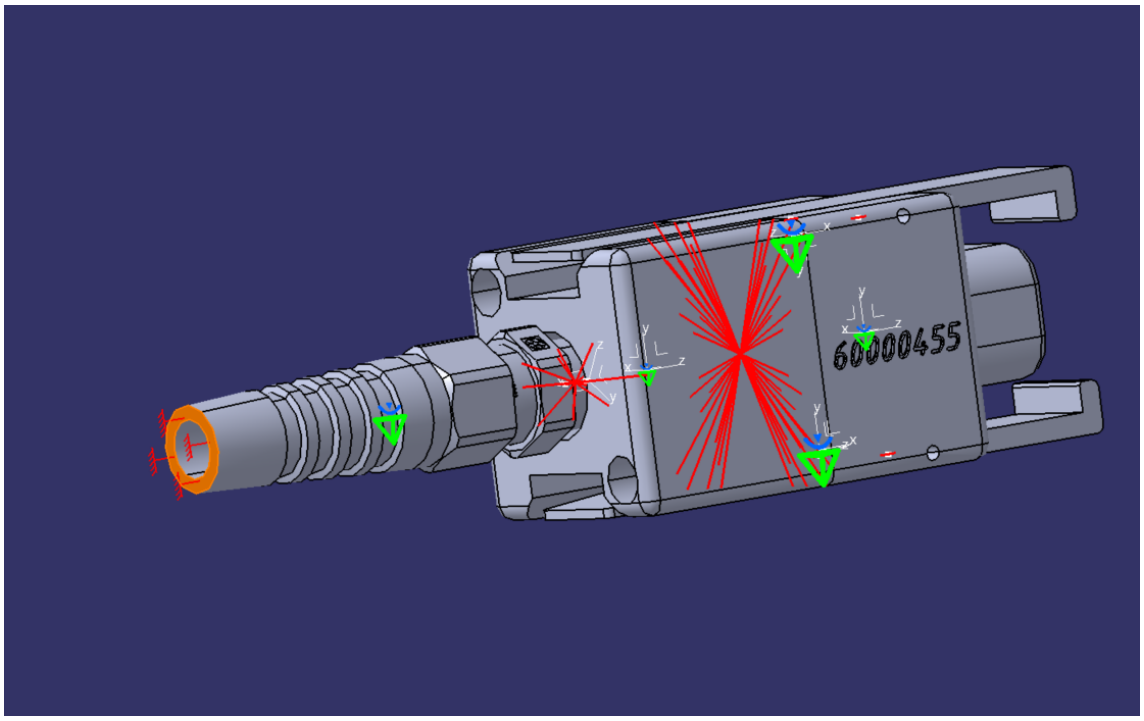

Figure 3.13: Clamped boundary condition.

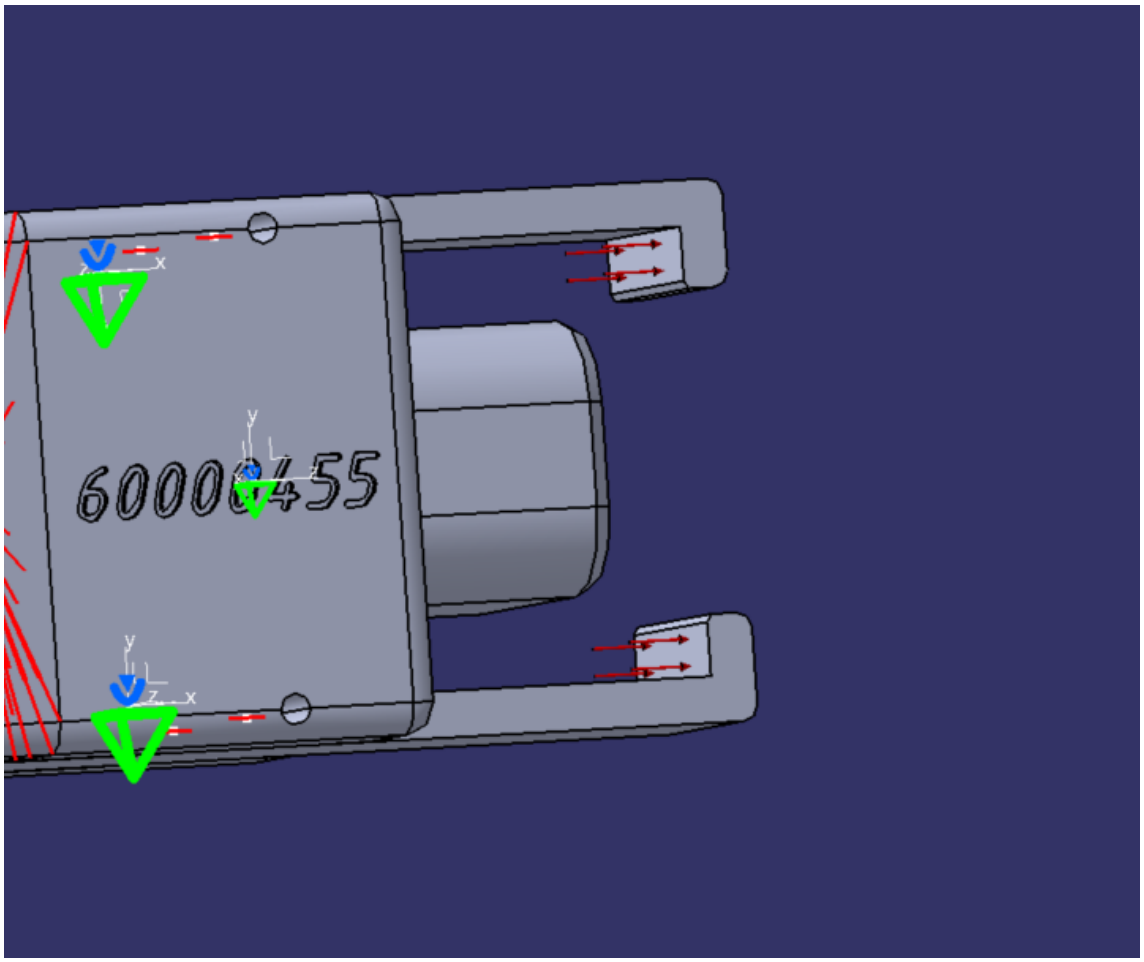

Figure 3.14: Distributed force boundary condition.

To study more clearly where the stress concentrations occurred, a local mesh was applied to the clamps. Figure 3.15 shows where the local mesh was implemented. To decide on the appropriate size of the local mesh, a mesh sensitivity study was performed. A mesh sensitivity analysis makes it possible to find a balance between avoiding unnecessary computational cost and obtaining a converged solution. The local mesh result was iterated with different mesh sizes to find the optimal mesh. As a metric for comparison between the mesh sizes, the maximum von Mises stress is chosen.

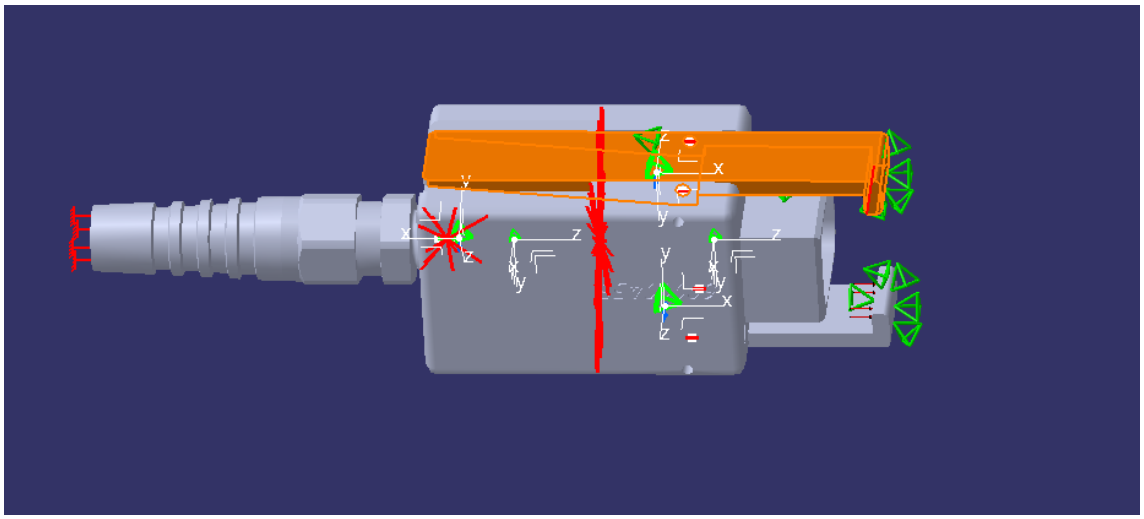

Figure 3.15: Selected surfaces where a local mesh was added are highlighted orange.

Since the connector is printed with 100% infill, the connector becomes solid and can be simulated in the same way as the purchased connector. Two types of FEA simulations were performed for the 3D printed connectors, one in which the entire connector except for the shafts was made of plastic material, and the other type of calculations where only the connector housing was made of 3D printed material and the clamps were made of steel similar to the purchased one.

4

Results

4.1 Material investigation

Three test specimens were printed and tested in each material. The material data obtained, see Table 4.1, from the tensile test are a mean value of all tests that were valid, which means that the test was performed correctly and that the sample did not slip during the test. All PLA test specimens cracked before the yield stress was found and all test specimens cracked before Poisson's ratio was found.

Table 4.1: Material data from tensile testing 3D printed test specimens.

Material	$E\ [MPa]$	$\sigma_y\ [MPa]$	$\nu\ [\ ]$
Sustarine	5101	32	-
PLA	2383	-	-
PLA-CF	5201	47	-
PETG	1478	39	-
PETG-CF	5317	22	-
PATH-CF	2993	34	-
TPU	62	9.13	-

A connector component was printed in each material, with the exception of PATH-CF. This material was excluded because of the challenges in achieving acceptable print settings and the poor surface quality that it produced, which made it unsuitable for printing connectors. After the different materials were printed, several visual observations were made regarding the printability and surface quality. PLA and PETG were the easiest to print and showed consistent results throughout the process. Both materials produced clean surfaces where the layers bonded well and had accurate hole geometries without the need for significant parameter adjustments in the slicer. PLA-CF and PETG-CF resulted in finer, more matte surface finishes because of the carbon fiber, which contributed to a more technical appearance. However, these materials showed a poorer result around small holes. ,see Figure 4.1. TPU required a print speed roughly half that of the other materials. Issues such as deformation in corners, holes, and insufficient layer bonding were observed; see Figure 4.2. PATH-CF had a noticeably rougher surface finish compared to the other materials; see Figure 4.3

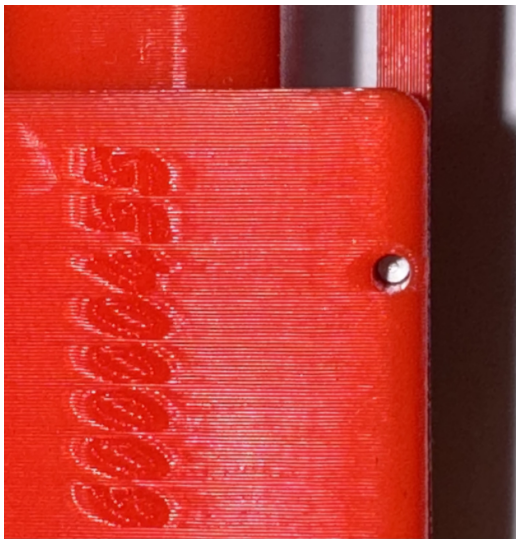

(a) PLA.

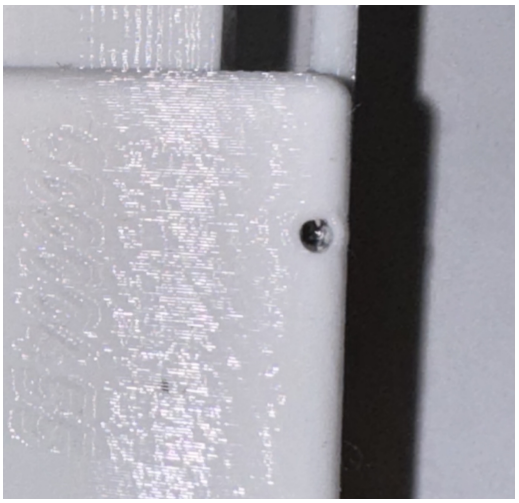

(b) PETG.

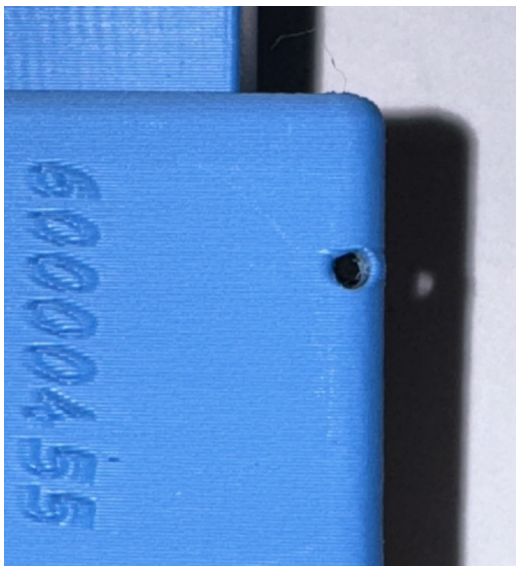

(c) PLA-CF.

(d) PETG-CF.

Figure 4.1: Surface printing results for PLA, PETG, PLA-CF and PETG-CF.

(a) (b)

Figure 4.2: Observed issues from printed TPU, (a) deformation in corners and holes, and (b) insufficient layer bonding.

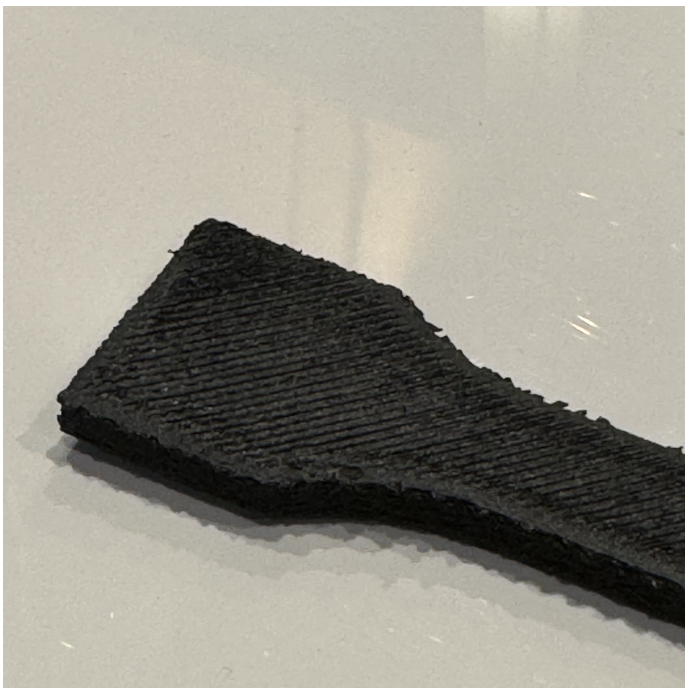

Figure 4.3: Surface of a 3D printed test specimen in PATH-CF.

4.2 Tensile test purchased connector

In Figure 4.4, a graph visualizes the load-deformation curve for the connector. The maximum force the connector could withstand before it detached from the adapter was 213.9 *N*, see Appendix .3 for raw data.

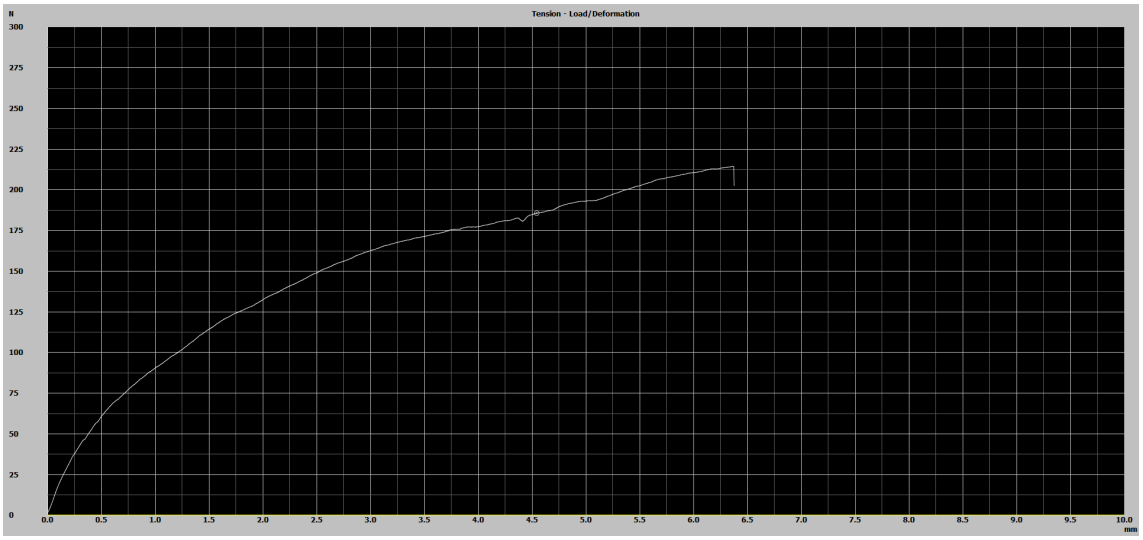

Figure 4.4: Force versus pull-out displacement required for the connector to detach from the adapter.

4.3 Finite Element analysis results

This part of the report presents the findings of the FEA simulations. This includes mesh sensitivity analysis, FEA on purchased connectors, and 3D printed connectors.

4.3.1 Mesh sensitivity

This section shows the results of the local mesh sensitivity analysis; the local mesh size with associated von Mises stress is shown in Table 4.2. At a mesh size of 0.25 mm, a clear trend could be observed where the von Mises stress started to increase rapidly compared to previous mesh sizes. This indicates that the model is approaching a singular behavior in the area where the force is applied. When the mesh was refined to 0.0625 mm, an error occurred in the simulation, confirming that a singularity had occurred. Consequently, a 0.5 mm local mesh size was chosen as it offers a balance between numerical stability and solution accuracy, lying just before the point where the results begin to diverge due to over-refinement. Figure 4.5 shows a visual representation of the stress concentration for some of the different iterations.

Table 4.2: Mesh sensitivity analysis showing von Mises stress for different local mesh sizes.

Local mesh size [mm]	von Mises stress [Pa]
8	$2.16{\cdot}10^7$
4	$2.22{\cdot}10^7$
2	$2.10{\cdot}10^7$
1	$2.43{\cdot}10^7$
0.5	$2.59{\cdot}10^7$
0.25	$3.55{\cdot}10^7$
0.125	$4.80{\cdot}10^7$
0.0625	-

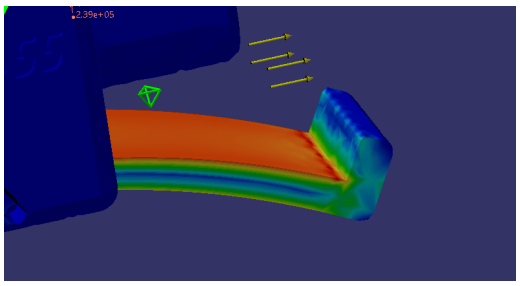

(a) Local mesh size 2mm.

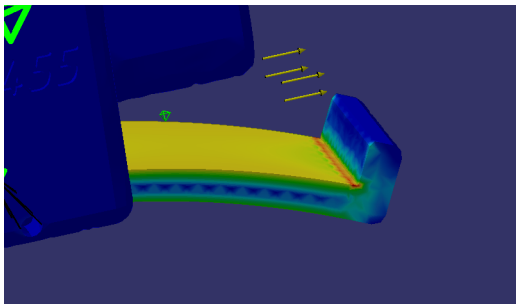

(b) Local mesh size 1mm.

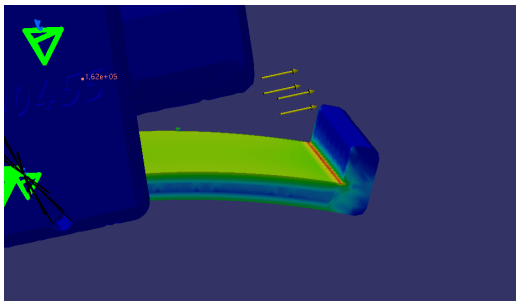

(c) Local mesh size 0.5mm.

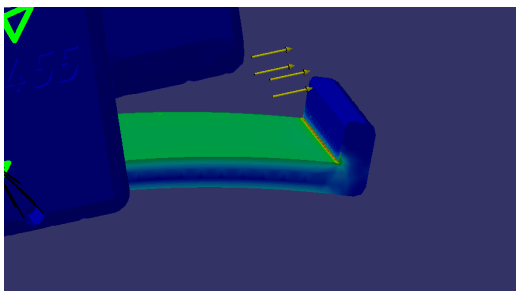

(d) Local mesh size 0.25mm.

Figure 4.5: Comparison between a local mesh of 2,1,0.5,0.25 mm respectivaly.

4.3.2 FEA results purchased connector

When applying a distributed force with a magitude of 213.9N the maximum von Mises stress for the purchased connector was 25,9 MPa. The simulation results can be seen in Figures 4.6 and 4.7.

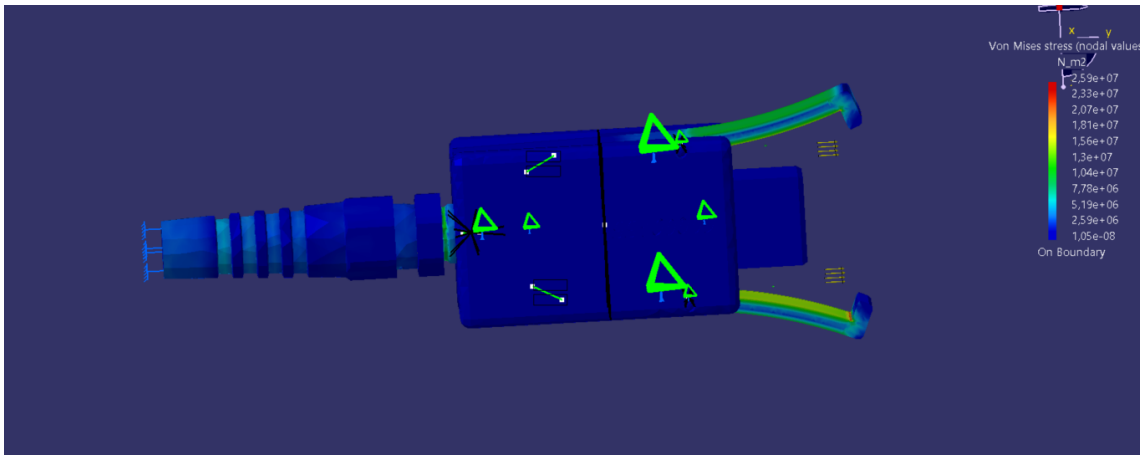

Figure 4.6: Result of FEA simulation of the purchased connectorfrom the side.

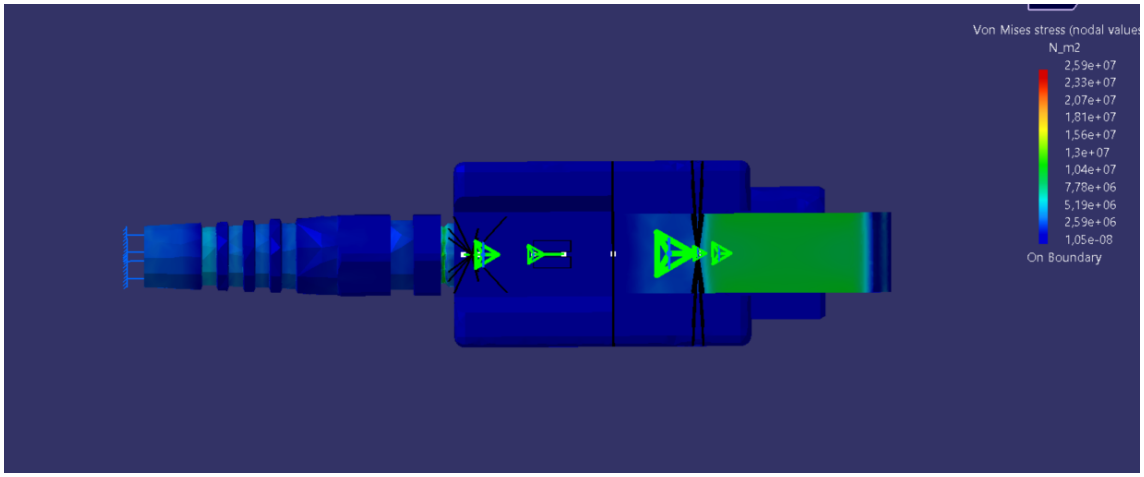

Figure 4.7: Result of FEA simulation of the purchased connector from above.

4.3.3 Finite Element Analysis results 3D printed connectors

The von Mises stress results for the 3D printed connectors when loaded with a force of 213.9 N has been gathered in a table, see Table 4.3. From the table it can be seen that the simulations, in which only the housing was simulated with the 3D printed material and the metal clams, gave the same results. For a visual representation of the simulation results,see Figures 4.8 and 4.9, for larger pictures, see Appendix .4.

Table 4.3: von Mises stress results from simulating the different 3D printed materials.

Material	von Mises stress [Pa]
PLA (all parts)	$2.67 \cdot 10^7$
PLA (only housing)	$2.59 \cdot 10^7$
PLA-CF(all parts)	$2.69 \cdot 10^7$
PLA-CF (only housing)	$2.59 \cdot 10^7$
PETG(all parts)	$2.61 \cdot 10^7$
PETG (only housing)	$2.59 \cdot 10^7$
PETG-CF(all parts)	$2.72 \cdot 10^7$
PETG-CF (only housing)	$2.59 \cdot 10^7$
TPU(all parts)	$2.54 \cdot 10^7$
TPU (only housing)	$2.59 \cdot 10^7$
PATH-CF (all parts)	$2.69 \cdot 10^7$
PATH-CF (only housing)	$2.59 \cdot 10^7$

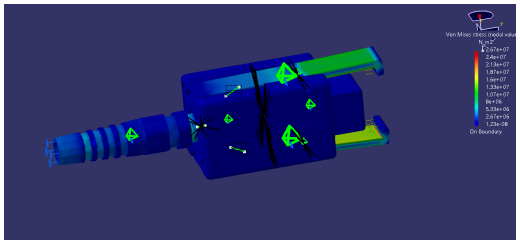

(a)PLA, von Mises stress: $2.67 \cdot 10^7 Pa$

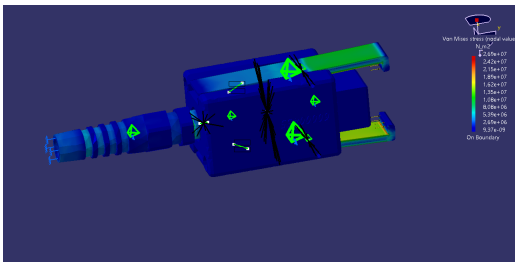

(b) PLA-CF, von Mises stress: $2.69 \cdot 10^7 Pa$

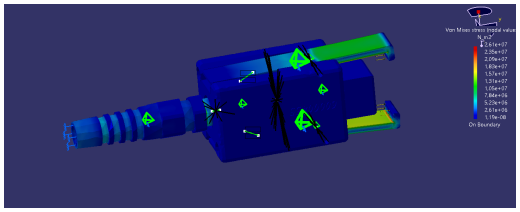

(c) PETG, von Mises stress: $2.61 \cdot 10^7 Pa$

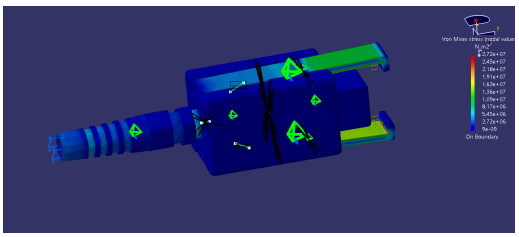

(d) PETG-CF, von Mises stress: $2.72 \cdot 10^7 Pa$

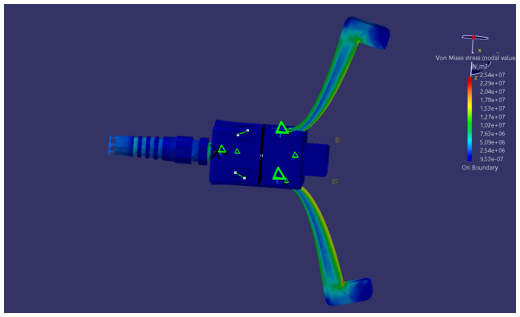

(e) TPU, von Mises stress: $2.54 \cdot 10^7 Pa$

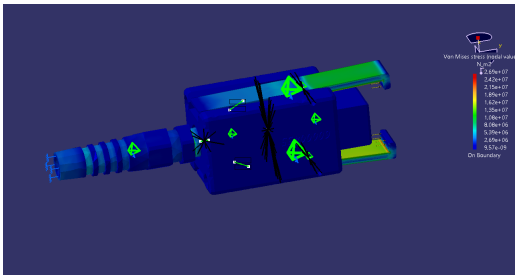

(f) PATH-CF, von Mises stress: $2.69 \cdot 10^7 Pa$

Figure 4.8: FEA simulations for the 3D printed materials.

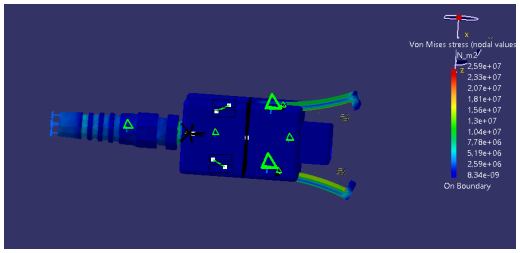

(a)PLA, von Mises stress: $2.59 \cdot 10^7 Pa$

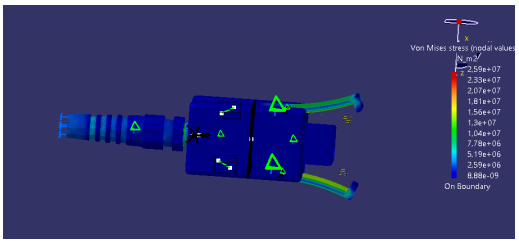

(b) PLA-CF, von Mises stress: $2.59 \cdot 10^7 Pa$

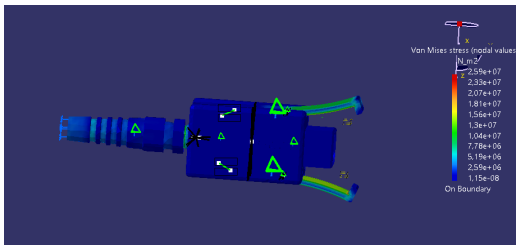

(c) PETG, von Mises stress: $2.59 \cdot 10^7 Pa$

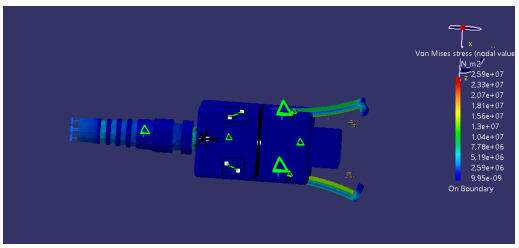

(d) PETG-CF, von Mises stress: $2.59 \cdot 10^7 Pa$

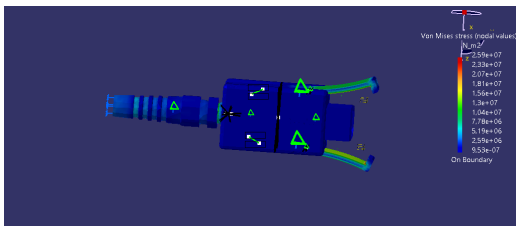

(e) TPU, von Mises stress: $2.59 \cdot 10^7 Pa$

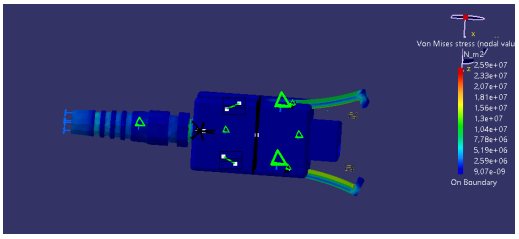

(f) PATH-CF, von Mises stress: $2.59 \cdot 10^7 Pa$

Figure 4.9: FEA simulations for the 3D printed materials with metal clams.

5
Discussion and Conclusion

In this section, results and suggestions on follow-up studies will be discussed.

5.1 Material data

The results of the tensile test on the test specimens presented in Table 4.1 differ from the material data provided by the manufacturer, Table 2.1, 2.2, 2.3 and 2.4. In particular, three of the materials, namely, Sustarine, PLA-CF, and PATH-CF, had extra large differences. A possible source of error for this is that different loading speeds may have been used during the testing. Something else that may have also affected this is whether the test specimen is mounted completely centered and straight in the machine during testing and whether the test specimen slipped during the test. For PLA-CF and PATH-CF, which were 3D printed, other printer settings may also have been used during the tests, and only three tests were conducted per material. An advantage of using the results of the tensile tests carried out in this project is that it can be ensured that the same printer settings were used during the tests as when the connectors were printed. However, the sources of error for mounting test specimens wrong and test machine settings are considered to be greater than the printer settings, and it was chosen to use the manufacturers material data for the simulations for all materials where possible.

5.2 3D printing and materials

In Section 4.1 some results regarding printability and surface quality were obtained. After the test specimens were printed, connectors were also printed in all materials except PATH-CF. PATH-CF had challenges in achieving acceptable print settings and resulted in rough surface quality; it was removed from further investigation. The next material that could be excluded was TPU as it needed much longer printing time, insufficient layer bonding, and deformation in corners as a result of challenging printer settings. That leaves PLA, PLA-CF, PETG and PETG-CF as options. All four materials were easy to print and had consistent results. The carbon fiber-infused materials resulted in a better surface finish but led to a poorer result around small holes. However, this is not considered a problem for the selected connector-design as the holes that were affected could be drilled instead. As a follow-up study, it is of interest to investigate other materials and other printer settings, such as comparing different infill structures and infill percentages. Something that could also be studied further is to perform physical tensile tests on the 3D printed contacts, similar to

what was done for the purchased contact, to see if they behave as expected. This could not be done in this project, as there was no suitable way to attach the 3D printed contacts to the test machine.

It is also worth noting that production has had problems with materials containing carbon fiber being conductive. This has led to contacts becoming hot during use, which should be avoided. The resistance was therefore measured with a multimeter on the 3D printed test specimens, but no conductive properties were found. Therefore, the carbon fiber-containing materials investigated during this study are considered suitable.

5.3 Finite Element Analysis

The results of the FEA simulation on the purchased connector are considered good, since the simulation confirmed the behavior that was shown during the physical test, and therefore the simulation setup was considered appropriate to use when studying the 3D printed materials. For all simulations, the stress concentrations emerged in the inner corner of the clamps, and the von Mises stress only reached its yield stress value for connector with the material TPU. This indicates that all other materials could be appropriate for printing the connector. From the results it can also be seen that all simulations in which metal clams were used gave the same results, see Table 4.3. This is considered reasonable since the stress concentration is on the clams. If the connector was to be used as a spare part, an option could be to purchase metal clamps to assemble and only print the connector housing.
To be able to know if a 3D printed connector could have completely replaced a purchased connector, more studies would have needed to be done, such as fatigue analysis, material wear, and a field study where the connector is tested over time in the factory. Other follow-up studies could be to investigate how the connector would react in different load cases, for example, a load case with side loads. The design of the connector is also something to investigate. A different placement of the shaft between the connector housing and the clam would lead to different forces, and the connector may behave differently and may be able to withstand more force before attaching from the adapter.

5.4 Sustainability

As mentioned in Section 2.5 3D printing as a manufacturing method can offer a more sustainable alternative to traditional machining, particularly due to its potential to reduce material waste. Furthermore, biodegradable materials such as PLA are available for use in 3D printing, which contributes to its environmental benefits. However, as mentioned in Section 2.4.1, it is important to recognize that certain advanced materials, such as carbon fiber-reinforced polymers, have significant challenges in terms of recyclability.

5.5 Fulfillment of aim and goals

The thesis was divided into different problem areas; see Section 1.4 that should be met to carry out the work. This Section will discuss the fulfillment of the problem areas.

The first goal was to examine which material was suitable for 3D printed connectors through tensile testing and to evaluate the ease of printing and printing results. This goal is considered to be achieved; see Section 5.2. The second goal was to investigate what parts of the connector are suitable for 3D printing. As discussed in Section 5.3, the results suggest that it would be feasible to 3D print the entire connector, or an option could be to only print the connector housing and assemble the connector using purchased metal clams. Based on the discussion, the goal is considered to have been met. The third goal, which type of load case should be investigated, is considered to be fulfilled; see Section 2.1. The fourth goal was to investigate 3D printed connectors during the selected load case by performing finite element analysis and physical tests. Tensile tests were performed on the purchased connector and FEA simulations were done on the connector in the 3D printed materials. However, no physical tests could be performed on the 3D printed connectors, see Section 5.2, therefore this goal is considered to be partially achieved.

The fifth goal was to examine whether the FEA matches the physical testing of the 3D printed connectors. As mentioned in Section 5.2, there was no suitable way to attach the 3D printed connectors to the test machine, so no tests were performed. Therefore, this goal is considered not to have been achieved. The sixth goal was to compare the stresses of the purchased and 3D printed connectors that occurred during the selected loadcase. From the FEA results, the stresses were compared and, therefore, this goal is considered fulfilled. The last goal was to investigate how the chosen material and 3D printing as a manufacturing method affect the environment compared to the machined connector, and this was discussed in Section 5.4, the goal is considered fulfilled.

5.6 Conclusion

From this study, it can be seen that there are four materials that could be suitable for 3D printing connectors, PLA, PLA-CF, PETG, and PETG-CF for use as spare part. However, further studies are needed to determine whether 3D printed contacts can replace existing ones over a longer period of time.

Bibliography

[1] I. Gibson, D Rosen, B Stucker and M. Khorasani (2021) Additive Manufacturing Technologies. DOI: https://doi.org/10.1007/978-3-030-56127-7

[2] Ottosen, N. S. & Petersson, H. (1992) *Introduction to the finite element method*. Prentice Hall.

[3] J. Faludi, C. Bayley, S. Bhogal, and M. Iribarne (2015) Comparing environmental impacts of additive manufacturing vs traditional machining via life-cycle assessment *Rapid Prototyping Journal*, vol. 21, no. 1, pp. 14–33, 2015. DOI: 10.1108/RPJ-07-2013-0067

[4] M. Shuaib, A. Haleem, S. Kumar, M. Javaid, "*Impact of 3D Printing on the environment: A literature-based study*", Sustainable Operations and Computers, Volume 2, Pages 57-63,(2021), DOI: https://doi.org/10.1016/j.susoc.2021.04.001

[5] Hannan, A.N., Seidlitz, H., Hartung, D. et al. "*Sustainability and Circular Economy in Carbon Fiber-Reinforced Plastics*. Mater Circ Econ 6, 26 (2024). DOI: https://doi.org/10.1007/s42824-024-00111-2

[6] M. Ateeq, "*A state of art review on recycling and remanufacturing of the carbon fiber from carbon fiber polymer composite,* Composites Part C: Open Access, Volume 12, (2023), DOI: https://doi.org/10.1016/j.jcomc.2023.100412.

[7] Chalmers tekniska högskola, "*Regler för användning av AI-verktyg*," Chalmers.se, 2024. [Online]. Available: https://www.chalmers.se/utbildning/dina-studier/kandidat-och-examensarbete/regler-for-anvandning-av-ai-verktyg/. [Accessed: May 29 2025].

[8] Add North AB, Add North AB [Online]. Available: https://addnorth.com/ [Accessed: May 29, 2025].

[9] Marco, V., Massimo, G. Manuela, G. *"Additive manufacturing of flexible thermoplastic polyurethane (TPU): enhancing the material elongation through process optimisation"*. Prog Addit Manuf 10, 2877–2891 (2025). DOI: https://doi.org/10.1007/s40964-024-00790-y

[10] Raise3D, "*3D Printing Temperature: The Importance of Getting It Right*," Raise3D Blog, Sep 15, 2024. [Online]. Available: https://www.raise3d.com/blog/3d-printing-temperature/. [Accessed: Jun. 4, 2025].

[11] Röchling Group, "*Technical Data Sheet Sustarin C ESD 60 PLUS*," 1, 2017-08-22.

[12] MatWeb, "*Overview - Nylon 6, Unreinforced*," MatWeb Material Property Data, [Online]. Available: https://asia.matweb.com/search/SpecificMaterialPrint.asp?bassnum=o2400 [Accessed: Jun 4 2025].

[13] L. Kuentz, A. Salem, M. Singh, M.C. Halbig, J.A. Salem "*Additive Manufacturing and Characterization of Polylactic Acid (PLA) Composites Containing Metal Reinforcements*," NASA Technical Reports Server, Jan. 2016. [Online]. Available: `https://ntrs.nasa.gov/api/citations/20160010284/downloads/20160010284.pdf` [Accessed: Jun 4 2025].

[14] "*Poisson's Ratio of Common Materials*," Matmake. [Online]. Available: `https://matmake.com/properties/poissons-ratio-of-common-materials.html` [Accessed: Jun 4 2025].

A

Appendix 1

.1 3D-print settings

.1.1 PLA

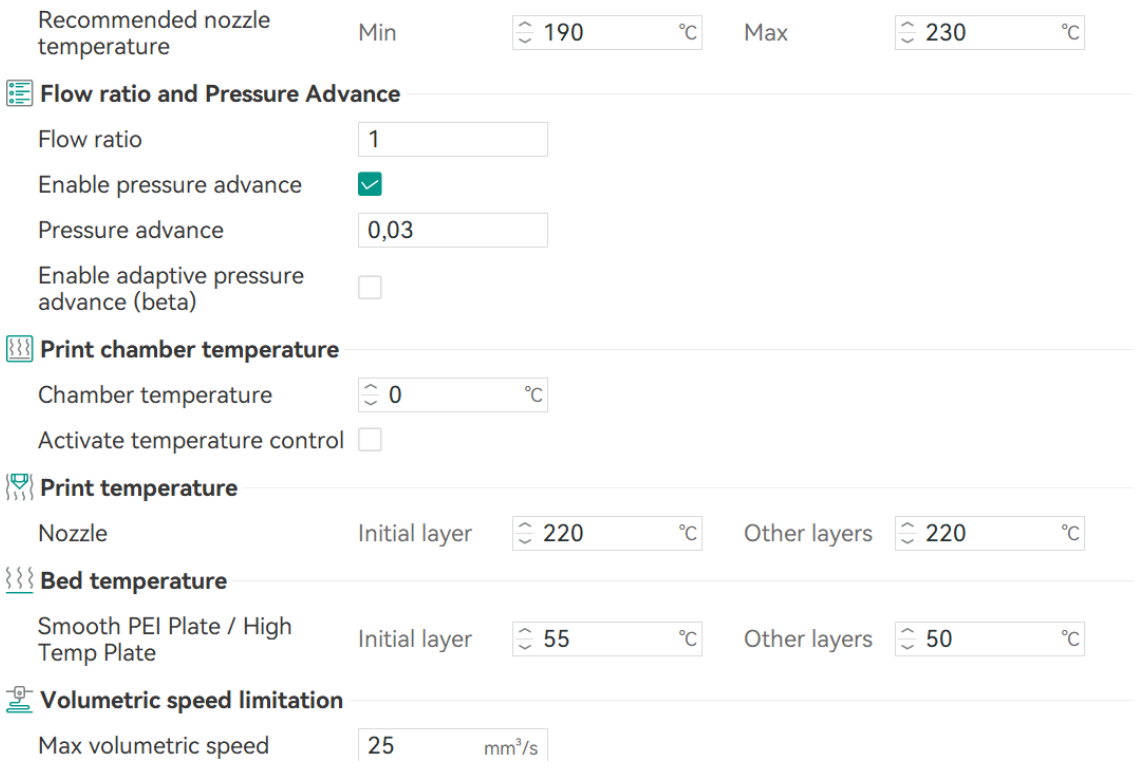

Figure .1: 3D print settings for PLA.

.1.2 PLA-CF

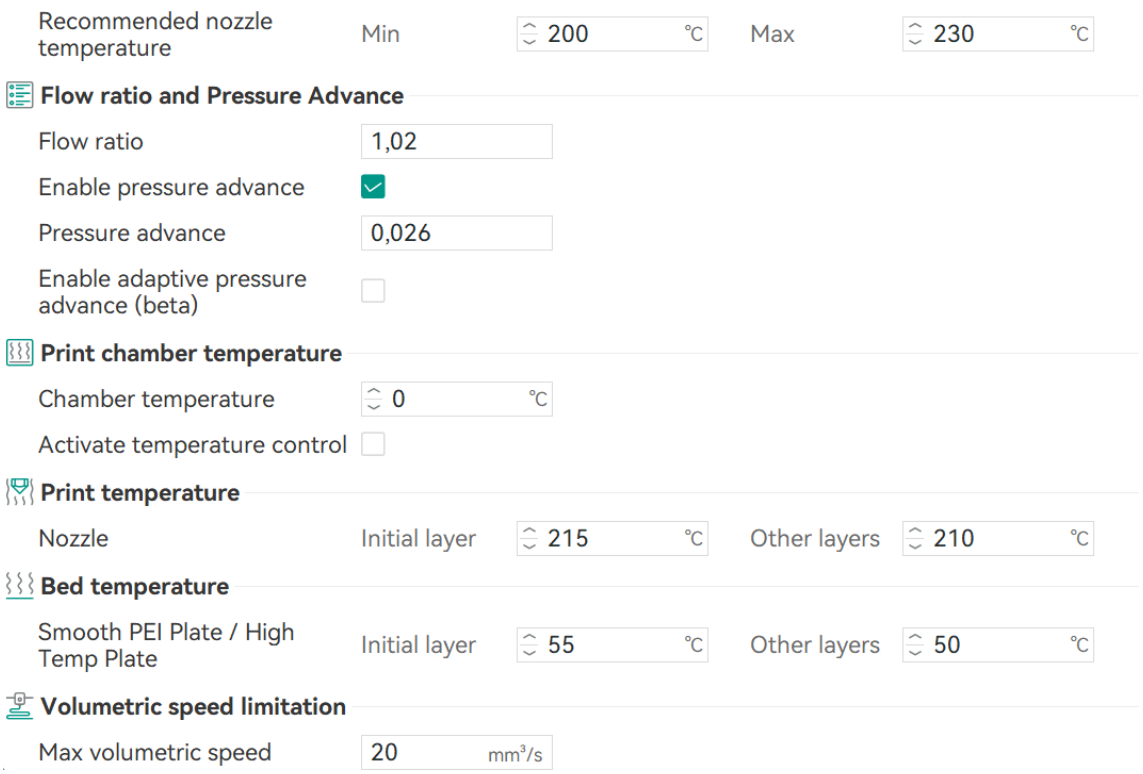

Figure .2: 3D print settings for PLA-CF.

.1.3 PETG

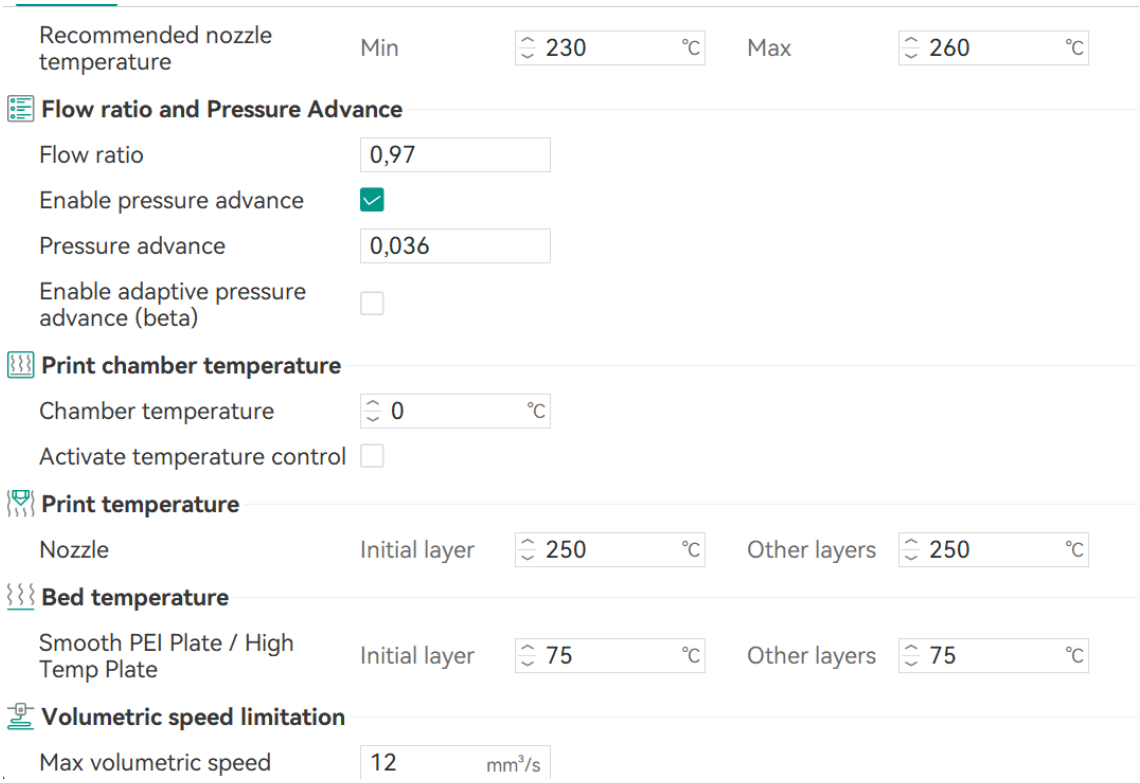

Figure .3: 3D print settings for PETG.

.1.4 PETG-CF

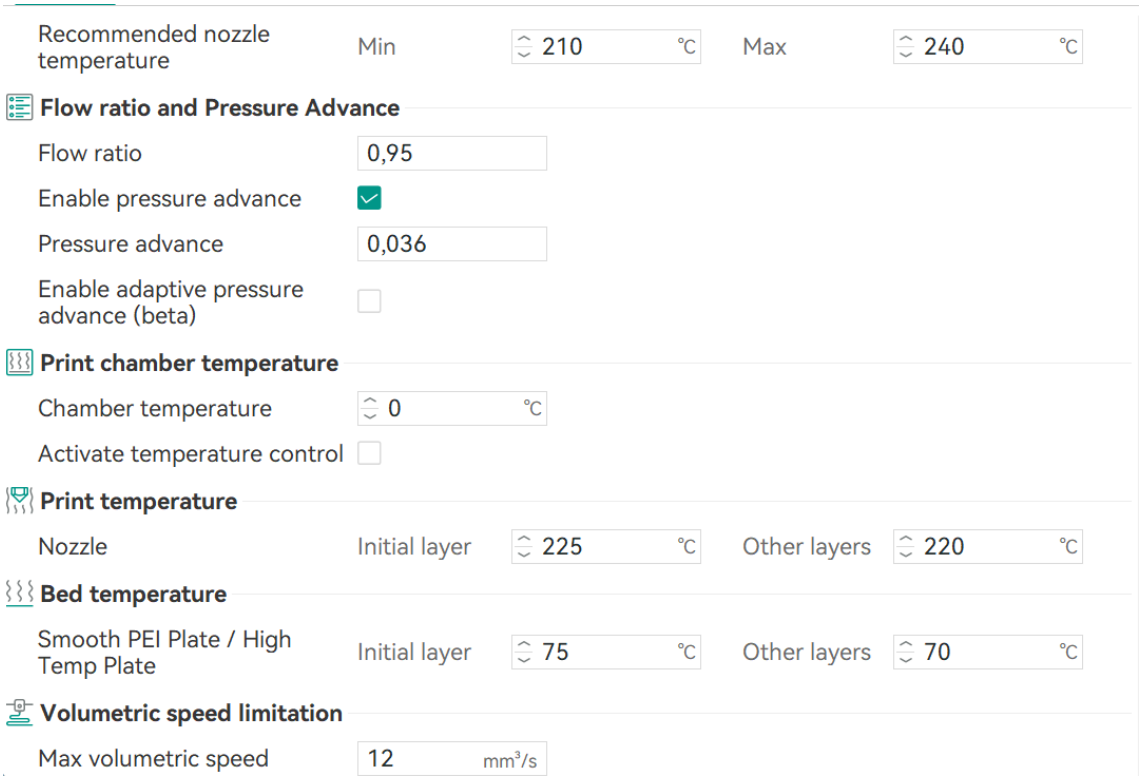

Figure .4: 3D print settings for PETG-CF.

.1.5 TPU

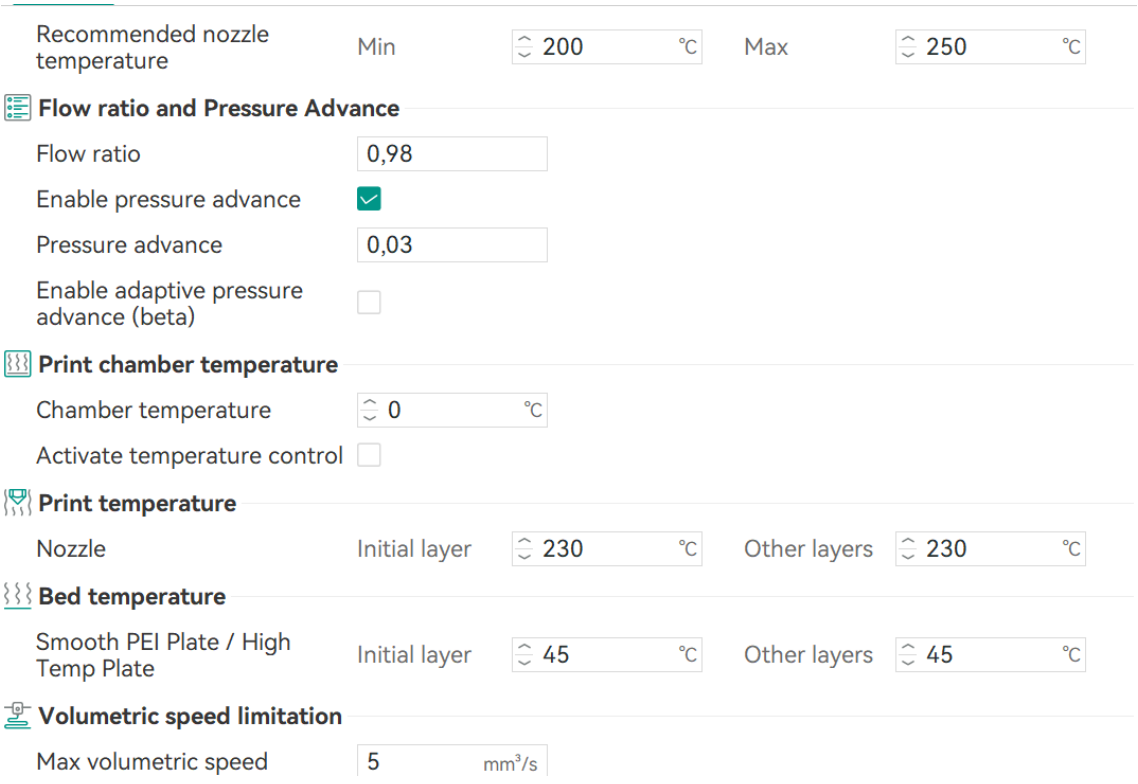

Figure .5: 3D print settings for TPU.

.1.6 PATH-CF

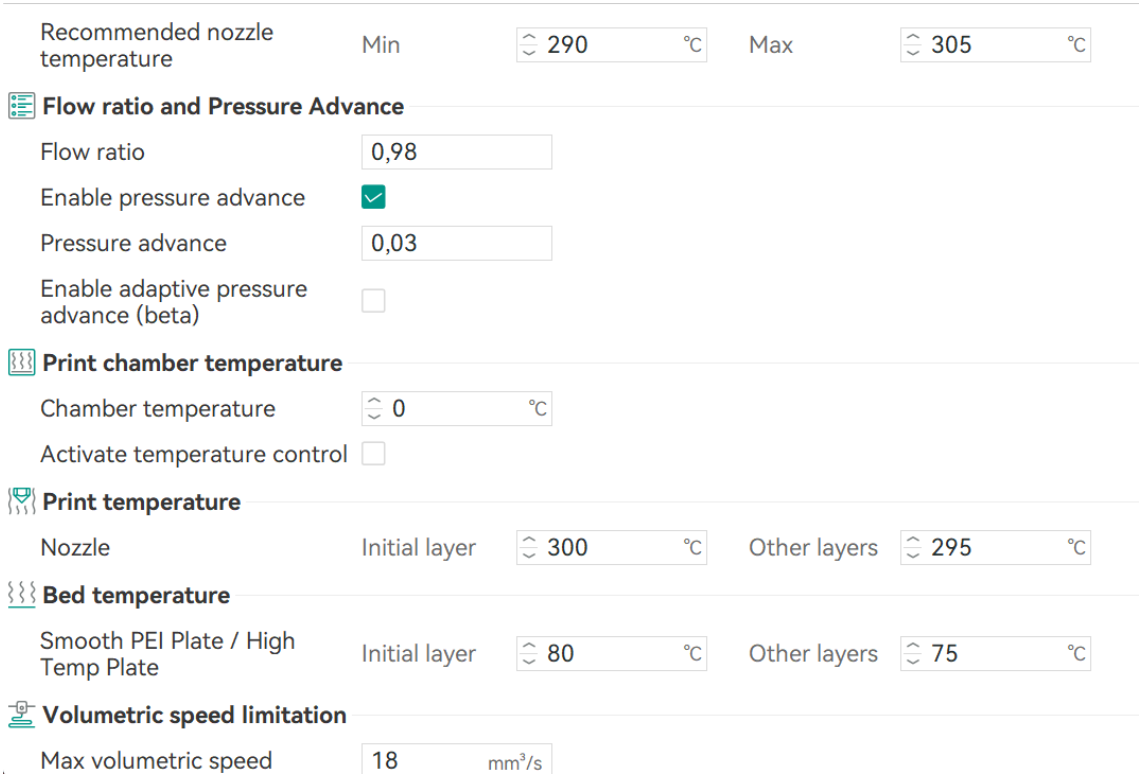

Figure .6: 3D print settings for PATH-CF.

.2 CAD drawing

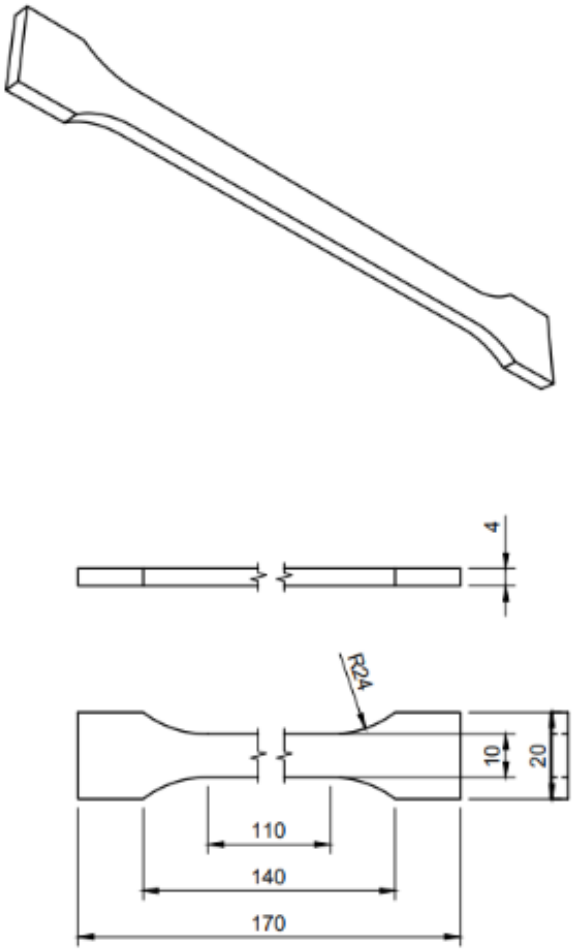

Figure .7: CAD drawing of test specimen.

.3 Tensile test purchased connector

Listing 1: Raw data from measurements, deformation in the left column, force in the right.

```
mm       N

0.000127314808196388     1.00527560710907
0.00516189122572541      1.74207961559296
0.013857813552022        2.86983823776245
0.0239244252443314       4.37571859359741
0.0340384989976883       6.08730459213257
0.0440861210227013       7.8343391418457
```

0.0540000163018703	9.66281795501709
0.0637675821781158	11.7328319549561
0.0738155394792557	13.4755458831787
0.0838523879647255	15.3594217300415
0.0939763486385345	16.9454746246338
0.104031287133694	18.599630355835
0.114290527999401	20.0844192504883
0.124048359692097	21.469596862793
0.134244680404663	22.9451103210449
0.145074665546417	24.4574699401855
0.155279248952866	25.8280353546143
0.165176823735237	27.0554065704346
0.175136238336563	28.3057746887207
0.185350373387337	29.5548725128174
0.195246294140816	30.803337097168
0.205323830246925	32.1704711914063
0.215468212962151	33.4970741271973
0.225355803966522	34.8511199951172
0.235517844557762	35.9534683227539
0.245757028460503	36.8846702575684
0.255669802427292	37.9189147949219
0.265764772891998	39.0648422241211
0.276056379079819	40.138599395752
0.28622642159462	41.1393013000488
0.296129137277603	42.3013648986816
0.306234121322632	43.3198547363281
0.316464394330978	44.363883972168
0.326193779706955	45.302074432373
0.330562204122543	45.6059951782227
0.347439616918564	46.3105239868164
0.35722890496254	47.2961082458496
0.367642164230347	48.4416542053223
0.377873033285141	49.4784393310547
0.387659400701523	50.5011215209961
0.398031800985336	51.3573608398438
0.407638430595398	52.2374839782715
0.417856097221375	53.4417304992676
0.427779078483582	54.3465042114258
0.43808525800705	55.2350158691406
0.446433812379837	55.9239158630371
0.463865607976913	56.8635063171387
0.473729819059372	57.7058944702148
0.483647018671036	58.6842308044434
0.494129806756973	59.755069732666
0.504052460193634	60.6640357971191
0.514431297779083	61.4384498596191
0.524172306060791	62.2288703918457
0.534286439418793	63.1308479309082
0.544478476047516	63.8527870178223
0.554477334022522	64.6021728515625
0.56441742181778	65.3127975463867
0.574227333068848	66.1771697998047
0.584184169769287	66.7447357177734
0.594064176082611	67.5113983154297
0.604516506195068	68.2875900268555
0.61447262763977	68.8654403686523

```
0.624817073345184       69.3463516235352
0.634580314159393       69.9538116455078
0.644674181938171       70.3734817504883
0.655023515224457       70.7803192138672
0.665104150772095       71.401123046875
0.675306856632233       72.1009521484375
0.685386121273041       72.7419509887695
0.69579005241394        73.2867736816406
0.705550253391266       73.9392166137695
0.715693473815918       74.576530456543
0.725838959217071       75.1785278320312
0.736105799674988       75.8711166381836
0.746120691299438       76.5240631103516
0.756331324577332       77.1030578613281
0.766468942165375       77.8248748779297
0.776429235935211       78.3395843505859
0.786572992801666       78.9688949584961
0.797166049480438       79.54052734375
0.807328283786774       79.888916015625
0.817276895046234       80.5809936523437
0.827423751354217       81.1625366210937
0.837503790855408       81.792610168457
0.847462773323059       82.3265075683594
0.857279598712921       83.0863037109375
0.87474662065506        83.6750869750977
0.884830236434937       84.2501525878906
0.895169675350189       84.8067855834961
0.90506899356842        85.2808380126953
0.91483861207962        85.7912216186523
0.925167798995972       86.5041427612305
0.935319721698761       87.0086822509766
0.945406794548035       87.5312728881836
0.955765962600708       87.788818359375
0.965659916400909       88.3449478149414
0.975628197193146       88.7379302978516
0.985903918743134       89.2964782714844
0.996118605136871       89.8147430419922
1.00600945949554        90.4166107177734
1.01630175113678        90.7234497070312
1.02607786655426        91.135498046875
1.03636884689331        91.462287902832
1.04670882225037        92.0104141235352
1.05654525756836        92.4727783203125
1.0665088891983 92.9369125366211
1.07729935646057        93.4109649658203
1.08757138252258        94.0247802734375
1.0972204208374 94.4341583251953
1.10730981826782        94.9214172363281
1.11758947372437        95.4198608398438
1.1275440454483 96.0216064453125
1.13781881332397        96.5933609008789
1.14784944057465        97.0068054199219
1.15813195705414        97.461799621582
1.16842615604401        97.7389068603516
1.17839431762695        98.1352005004883
1.18867242336273        98.6565170288086
```

```
1.19851386547089        99.0426406860352
1.20879936218262        99.452018737793
1.21894788742065        100.009544372559
1.22884953022003        100.447509765625
1.23913466930389        100.861968994141
1.24910032749176        101.296760559082
1.25943922996521        101.861907958984
1.26927089691162        102.396438598633
1.27935743331909        102.92626953125
1.28964340686798        103.329040527344
1.29972624778748        103.916046142578
1.30987048149109        104.538116455078
1.31964039802551        105.043418884277
1.32967102527618        105.456993103027
1.33975613117218        106.009819030762
1.35010814666748        106.375358581543
1.36006164550781        106.992858886719
1.37045860290527        107.642753601074
1.38092648983002        108.183258056641
1.39120304584503        108.729598999023
1.40134418010712        109.397033691406
1.41118037700653        109.863075256348
1.42127132415771        110.32772064209
1.43162560462952        110.65845489502
1.44158530235291        111.183074951172
1.45148956775665        111.58203125
1.46132719516754        112.026092529297
1.47173058986664        112.577651977539
1.48149704933166        113.136825561523
1.4914653301239 113.529052734375
1.50181818008423        113.884048461914
1.51159083843231        114.347938537598
1.52194249629974        114.718940734863
1.53172123432159        115.090461730957
1.54193949699402        115.554214477539
1.55196261405945        116.082649230957
1.56243312358856        116.582359313965
1.57238805294037        117.178771972656
1.58216464519501        117.582557678223
1.5925794839859 117.961822509766
1.60241627693176        118.419097900391
1.61231243610382        118.941047668457
1.62222051620483        119.282196044922
1.63211929798126        119.763748168945
1.64259970188141        120.113151550293
1.6524441242218 120.453918457031
1.6627368927002 120.754409790039
1.6727077960968 121.107116699219
1.68293750286102        121.397956848145
1.69290590286255        121.790306091309
1.70287299156189        122.201461791992
1.71309375762939        122.62825012207
1.72300255298614        122.958213806152
1.73335516452789        123.314353942871
1.75318384170532        123.806190490723
1.76315891742706        124.097915649414
```

```
1.77332031726837         124.458122253418
1.7834963798523 124.59635925293
1.79365873336792         124.943481445313
1.80407059192657         125.366577148438
1.82390403747559         125.786758422852
1.8340562582016 126.28736114502
1.8539502620697 126.753410339355
1.87135410308838         127.335327148438
1.88852143287659         127.641159057617
1.89836931228638         127.930465698242
1.90871620178223         128.373001098633
1.91868948936462         128.691787719727
1.92890381813049         129.215393066406
1.93887722492218         129.530883789062
1.94891023635864         129.908615112305
1.95919692516327         130.300079345703
1.96929180622101         130.703231811523
1.97945070266724         131.102188110352
1.98960769176483         131.530380249023
1.99989295005798         131.943176269531
2.00985646247864         132.409484863281
2.01982378959656         132.818725585938
2.02973103523254         133.170928955078
2.03969979286194         133.557189941406
2.04985976219177         133.939498901367
2.06015658378601         134.178237915039
2.06993341445923         134.577590942383
2.08042001724243         134.835388183594
2.09020209312439         135.155181884766
2.10036516189575         135.489974975586
2.12064409255981         135.911422729492
2.13061499595642         136.266174316406
2.14091110229492         136.515335083008
2.15074920654297         136.951141357422
2.16102910041809         137.447799682617
2.17087841033936         137.714492797852
2.18084955215454         138.063522338867
2.19074821472168         138.54621887207
2.20103645324707         138.917465209961
2.21082758903503         139.099792480469
2.22085928916931         139.495956420898
2.23083090782166         139.839019775391
2.2410581111908 140.168991088867
2.25141668319702         140.434158325195
2.26126050949097         140.783309936523
2.27155518531799         141.054824829102
2.28134393692017         141.274505615234
2.29176497459412         141.559371948242
2.30173563957214         141.917663574219
2.31158256530762         142.219436645508
2.32193613052368         142.564392089844
2.33222031593323         142.991806030273
2.34212946891785         143.317459106445
2.3519766330719 143.617568969727
2.36265277862549         143.895950317383
2.37294054031372         144.269622802734
```

```
2.38271474838257         144.710632324219
2.39268898963928         145.015197753906
2.4031081199646 145.327621459961
2.41294765472412         145.742218017578
2.4232337474823 146.143203735352
2.43320250511169         146.5283203125
2.44336748123169         146.836807250977
2.45353007316589         147.178970336914
2.46344184875488         147.463073730469
2.47391438484192         147.934204101562
2.49407267570496         148.251724243164
2.50385594367981         148.557159423828
2.51420545578003         148.961074829102
2.52430009841919         149.367782592773
2.53413891792297         149.795333862305
2.54417109489441         150.184005737305
2.55414724349976         150.457565307617
2.56431460380554         150.72819519043
2.5746111869812 150.97087097168
2.59488844871521         151.417984008789
2.60486173629761         151.73486328125
2.61502981185913         151.994064331055
2.62519264221191         152.335083007813
2.63555288314819         152.576232910156
2.6454586982727 152.949142456055
2.65555357933044         153.354721069336
2.66578483581543         153.621658325195
2.67569947242737         153.864212036133
2.68573832511902         154.150726318359
2.69583868980408         154.472808837891
2.71605563163757         154.870635986328
2.72622632980347         155.088531494141
2.74727010726929         155.496139526367
2.7571804523468 155.802093505859
2.77732944488525         156.264694213867
2.78762722015381         156.486038208008
2.79747366905212         156.799224853516
2.80770421028137         157.076721191406
2.81787180900574         157.343032836914
2.82822585105896         157.677825927734
2.83813381195068         158.022277832031
2.84835886955261         158.382995605469
2.85826539993286         158.746002197266
2.86811447143555         159.015747070313
2.87840533256531         159.346466064453
2.8986873626709 159.718109130859
2.90853404998779         160.024444580078
2.92881107330322         160.477401733398
2.93884444236755         160.847015380859
2.94882416725159         161.069488525391
2.96898317337036         161.376205444336
2.97927689552307         161.664367675781
2.99930167198181         162.078323364258
3.00966191291809         162.316818237305
3.01970267295837         162.577285766602
3.03966999053955         162.897720336914
```

```
3.06001114845276         163.34228515625
3.07024168968201         163.620162963867
3.08028626441956         163.820907592773
3.0904529094696 164.103866577148
3.10042929649353         164.374252319336
3.11103940010071         164.685028076172
3.12152743339539         164.922622680664
3.14130353927612         165.244583129883
3.15166831016541         165.417892456055
3.17157435417175         165.702377319336
3.19185137748718         166.15087890625
3.21181988716126         166.453414916992
3.23190784454346         166.876129150391
3.2422034740448 167.132781982422
3.26236462593079         167.408874511719
3.28258895874023         167.694381713867
3.29295444488525         167.854080200195
3.31298232078552         168.220397949219
3.33346009254456         168.524444580078
3.3533775806427 168.635101318359
3.37353515625   168.967361450195
3.38351011276245         169.25959777832
3.40366148948669         169.683578491211
3.42426609992981         169.992202758789
3.44418430328369         170.091186523438
3.46434903144836         170.314544677734
3.48450398445129         170.685302734375
3.49480605125427         170.843872070313
3.51509642601013         171.090362548828
3.5351984500885 171.300628662109
3.55637049674988         171.692352294922
3.57665753364563         171.992462158203
3.58670282363892         172.181655883789
3.60718679428101         172.388748168945
3.61717057228088         172.547073364258
3.63739609718323         172.816177368164
3.65756177902222         173.022125244141
3.66786217689514         173.205093383789
3.68801641464233         173.586517333984
3.69569897651672         173.892730712891
3.71325254440308         174.130706787109
3.72348785400391         174.337677001953
3.7334578037262 174.705123901367
3.75393557548523         175.008285522461
3.77372026443481         175.200012207031
3.78422379493713         175.201156616211
3.80421161651611         175.208282470703
3.8243899345398 175.224792480469
3.83468842506409         175.437606811523
3.84446716308594         175.809631347656
3.86500477790833         176.171249389648
3.8849093914032 176.474533081055
3.90520811080933         176.597900390625
3.92538619041443         176.618225097656
3.935387134552  176.515182495117
3.95530390739441         176.636901855469
```

```
3.97568082809448         176.538055419922
3.98592162132263         176.65901184082
4.00634288787842         176.856460571289
4.01613330841064         177.050979614258
4.03673696517944         177.37370300293
4.04805612564087         177.549179077148
4.06802749633789         177.812561035156
4.08838415145874         178.014709472656
4.0983624458313 178.256256103516
4.11846590042114         178.442764282227
4.12876272201538         178.684814453125
4.14899110794067         178.908432006836
4.15927934646606         179.274108886719
4.16925811767578         179.510299682617
4.1891598701477 179.856918334961
4.2094554901123 180.028442382813
4.22929954528809         180.282928466797
4.24952602386475         180.538452148438
4.26964092254639         180.552673339844
4.28987121582031         180.739959716797
4.31035327911377         180.983657836914
4.33024597167969         181.465194702148
4.34022092819214         181.756423950195
4.35051965713501         181.969360351562
4.37056398391724         182.085876464844
4.38116550445557         181.564559936523
4.39106845855713         181.014022827148
4.40109968185425         180.45280456543
4.4111123085022 180.179504394531
4.42102336883545         180.474533081055
4.43096494674683         181.269668579102
4.44097280502319         182.02653503418
4.45092058181763         182.732345581055
4.46087551116943         183.333572387695
4.47129392623901         183.654907226562
4.48139619827271         183.946365356445
4.49958562850952         184.19743347168
4.51178884506226         184.48649597168
4.52157783508301         184.700454711914
4.5316801071167 184.998275756836
4.54191637039185         185.185180664062
4.56310272216797         185.364196777344
4.58314275741577         185.544372558594
4.60375213623047         185.783233642578
4.62390518188477         186.18244934082
4.64444446563721         186.519271850586
4.66435718536377         186.700454711914
4.6746563911438 186.904006958008
4.69475984573364         187.084548950195
4.70492172241211         187.440689086914
4.71527194976807         187.831390380859
4.72549724578857         188.194900512695
4.7353367805481 188.604415893555
4.74524116516113         189.006286621094
4.75547456741333         189.235763549805
4.7654504776001 189.5146484375
```

```
4.78572988510132        189.930374145508
4.80587768554687        190.408996582031
4.82648229598999        190.717880249023
4.83627271652222        190.915710449219
4.85668897628784        191.185317993164
4.87742185592651        191.480224609375
4.89765214920044        191.670043945313
4.90801525115967        191.870666503906
4.92817115783691        192.224014282227
4.94808435440063        192.403030395508
4.96794271469116        192.44255065918
4.98856830596924        192.43391418457
5.00854587554932        192.596420288086
5.01884984970093        192.729705810547
5.03871297836304        192.697296142578
5.05902147293091        192.670623779297
5.07791948318481        192.799194335938
5.09452390670776        192.948364257813
5.1046929359436 193.192947387695
5.1149263381958 193.428009033203
5.13527202606201        193.804229736328
5.14556503295898        194.097213745117
5.16540384292603        194.436965942383
5.17569303512573        194.794128417969
5.18560266494751        195.109100341797
5.19583463668823        195.363220214844
5.20574808120728        195.628387451172
5.2260274887085 196.036102294922
5.23587322235107        196.362777709961
5.24610662460327        196.592239379883
5.25646352767944        196.88395690918
5.26624917984009        197.151153564453
5.28672456741333        197.491287231445
5.3070011138916 197.951232910156
5.31722497940063        198.325042724609
5.3375039100647 198.75373840332
5.34773063659668        199.08268737793
5.36890602111816        199.424850463867
5.37888431549072        199.671966552734
5.39923477172852        199.974243164062
5.40940284729004        200.233306884766
5.41938066482544        200.476119995117
5.43959379196167        200.934280395508
5.44982576370239        201.192459106445
5.46011638641357        201.519760131836
5.48003101348877        201.673248291016
5.50012874603271        201.95036315918
5.51029968261719        202.164321899414
5.52027082443237        202.516784667969
5.54080533981323        202.922988891602
5.55084753036499        203.15803527832
5.57081460952759        203.481658935547
5.58065938949585        203.817596435547
5.60081958770752        204.112991333008
5.61111783981323        204.323791503906
5.6212797164917 204.682723999023
```

```
5.63138198852539         204.975463867187
5.64173603057861         205.30517578125
5.65197324752808         205.48762512207
5.67193269729614         205.925216674805
5.69210004806519         206.106903076172
5.71201658248901         206.229263305664
5.72200727462769         206.284271240234
5.7334451675415 206.594543457031
5.75372982025146         206.931884765625
5.77414512634277         207.213439941406
5.79412317276001         207.368713378906
5.80410671234131         207.535034179687
5.82408142089844         207.745559692383
5.84449052810669         208.122787475586
5.86484479904175         208.364334106445
5.87482404708862         208.593536376953
5.8949933052063 208.743087768555
5.90522861480713         208.948669433594
5.92507553100586         209.164276123047
5.94535493850708         209.578735351562
5.96597003936768         209.733627319336
5.98632383346558         209.984817504883
6.00604963302612         210.103225708008
6.01648283004761         210.200424194336
6.03652477264404         210.358367919922
6.05675649642944         210.526580810547
6.07704257965088         210.842193603516
6.09706783294678         211.247131347656
6.10762214660644         211.443054199219
6.12777900695801         211.78889465332
6.13801431655884         211.991424560547
6.15818119049072         212.181625366211
6.16855049133301         212.28581237793
6.18853902816772         212.28581237793
6.19885349273682         212.255706787109
6.21865177154541         212.238677978516
6.23894357681274         212.467254638672
6.25909376144409         212.914108276367
6.27932929992676         213.023895263672
6.28950929641724         213.107376098633
6.30980539321899         213.264022827148
6.31966304779053         213.408111572266
6.34014940261841         213.576461791992
6.36011552810669         213.914947509766
6.3706316947937 213.722320556641
6.37522411346436         201.991012573242
```

.4 Figures simulated connector

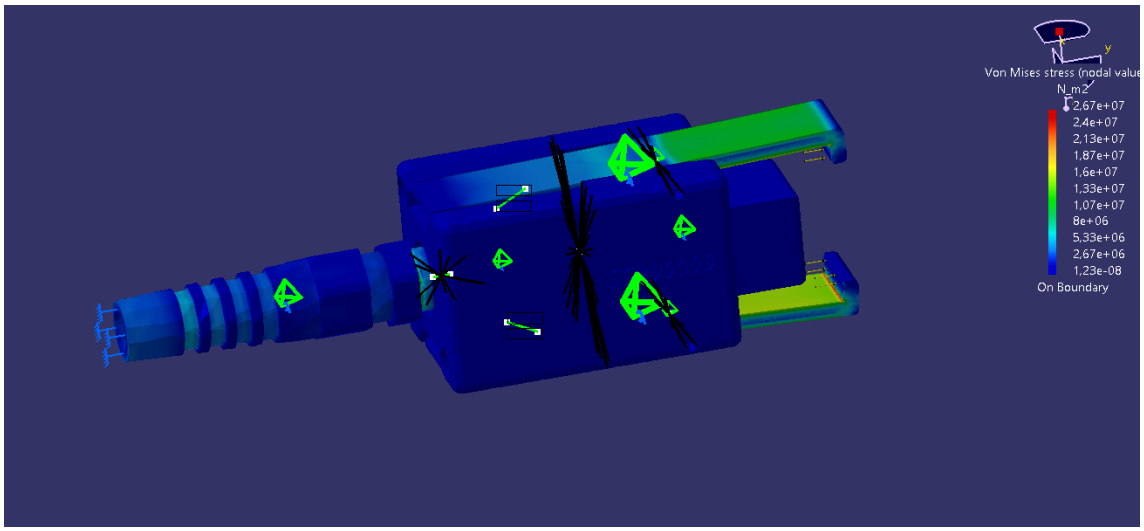

Figure .8: Connector in PLA

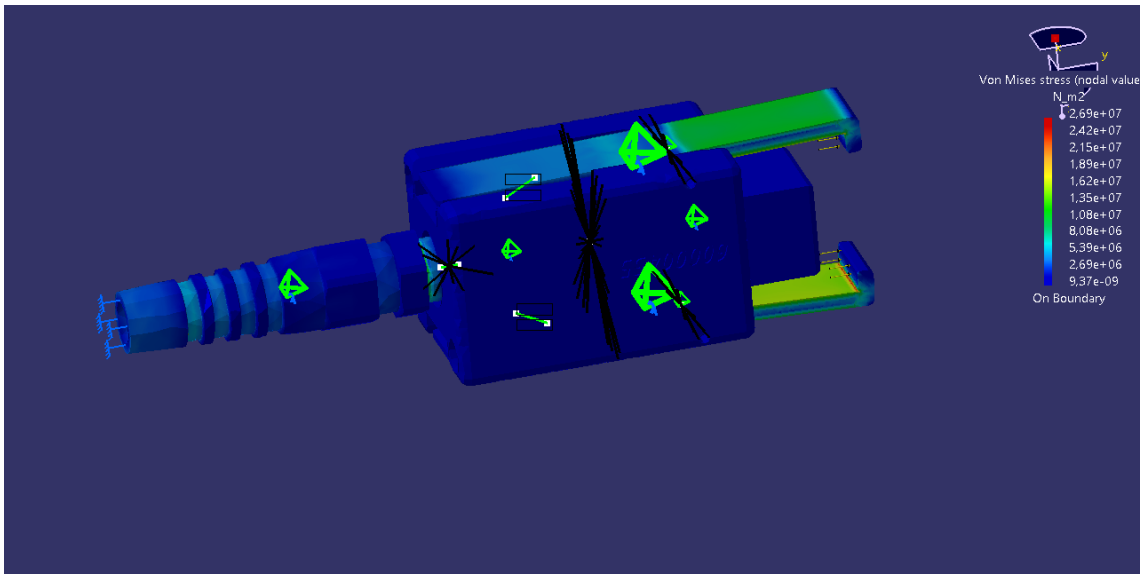

Figure .9: Connector in PLA-CF

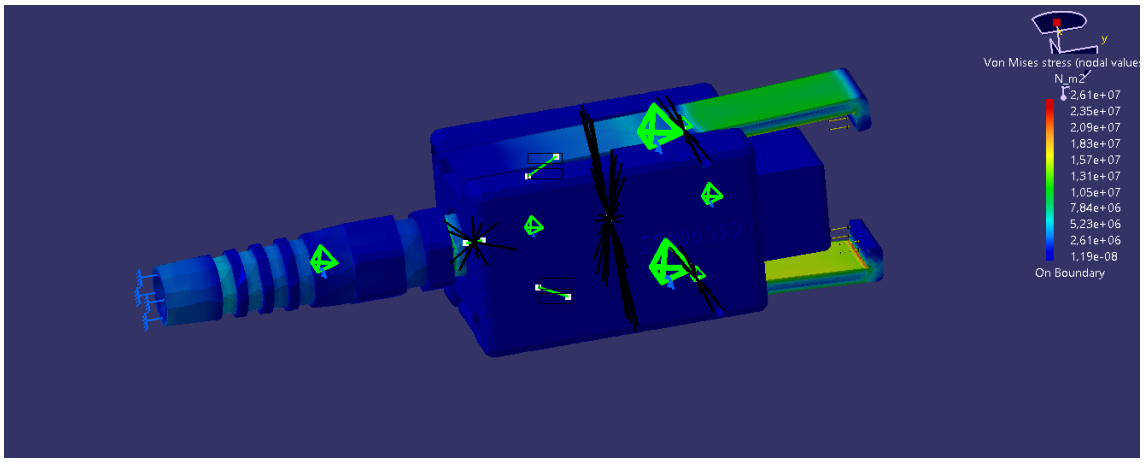

Figure .10: Connector in PETG

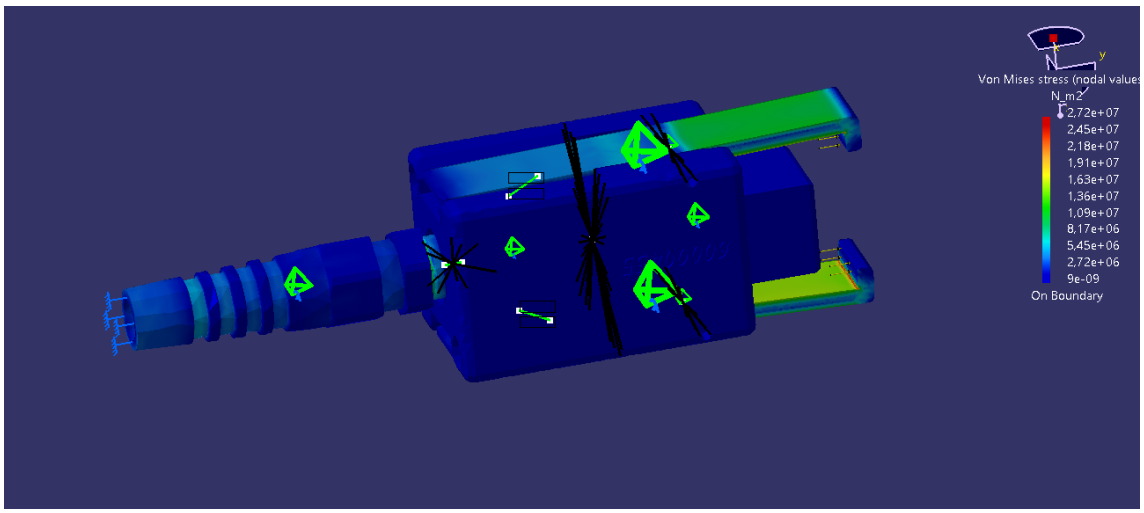

Figure .11: Connector in PETG-CF

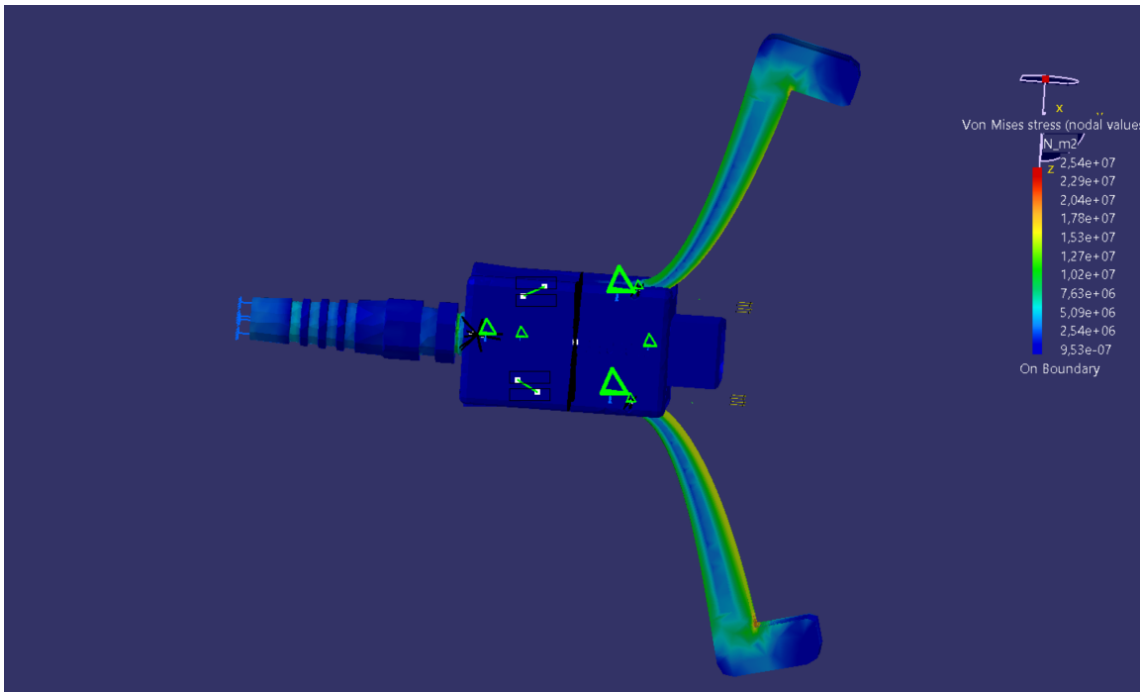

Figure .12: Connector in TPU

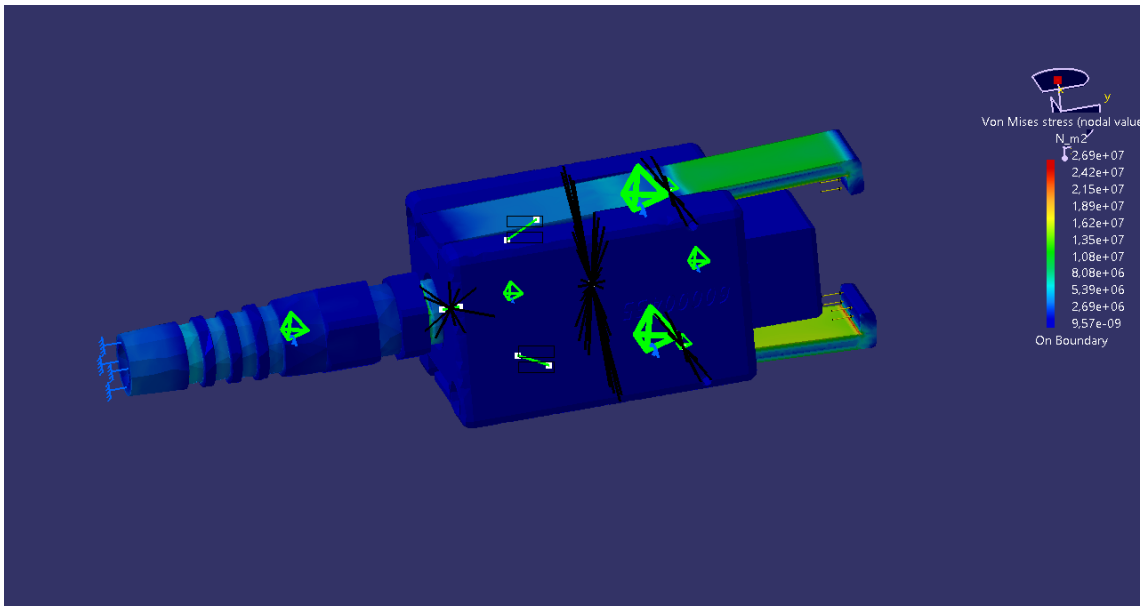

Figure .13: Connector in PATH-CF

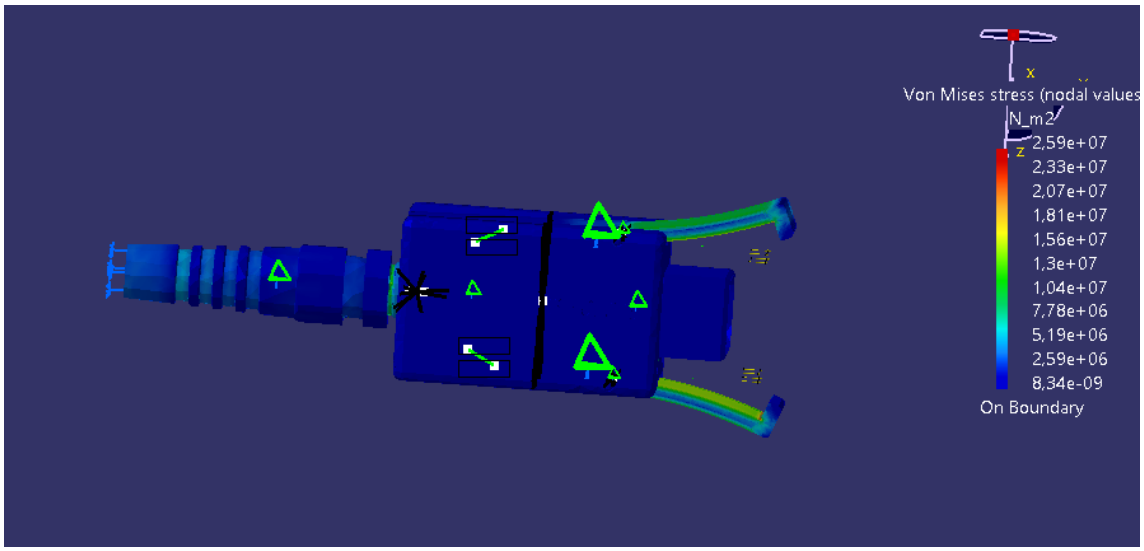

Figure .14: Connector in PLA except the clams.

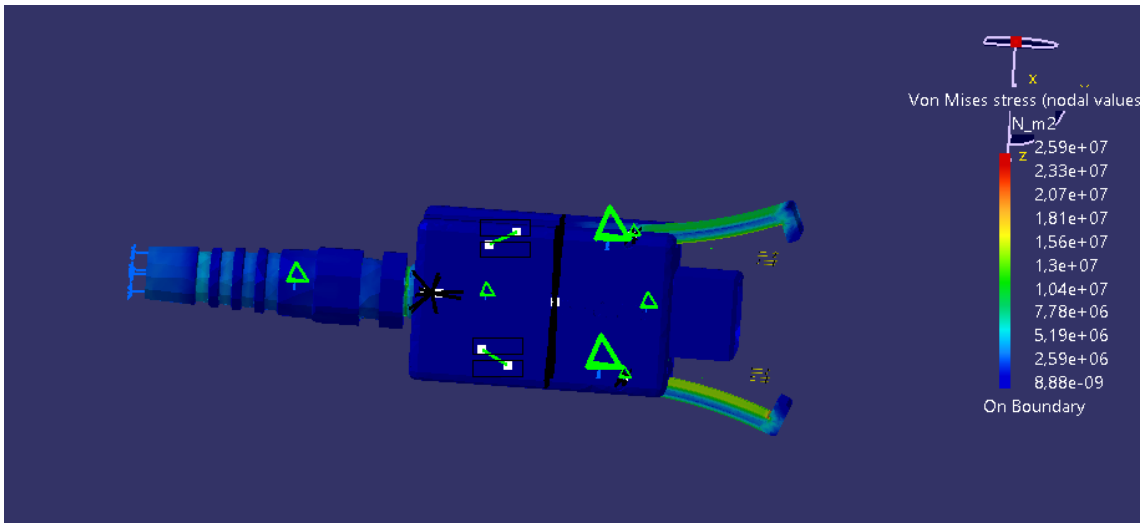

Figure .15: Connector in PLA-CF except the clams.

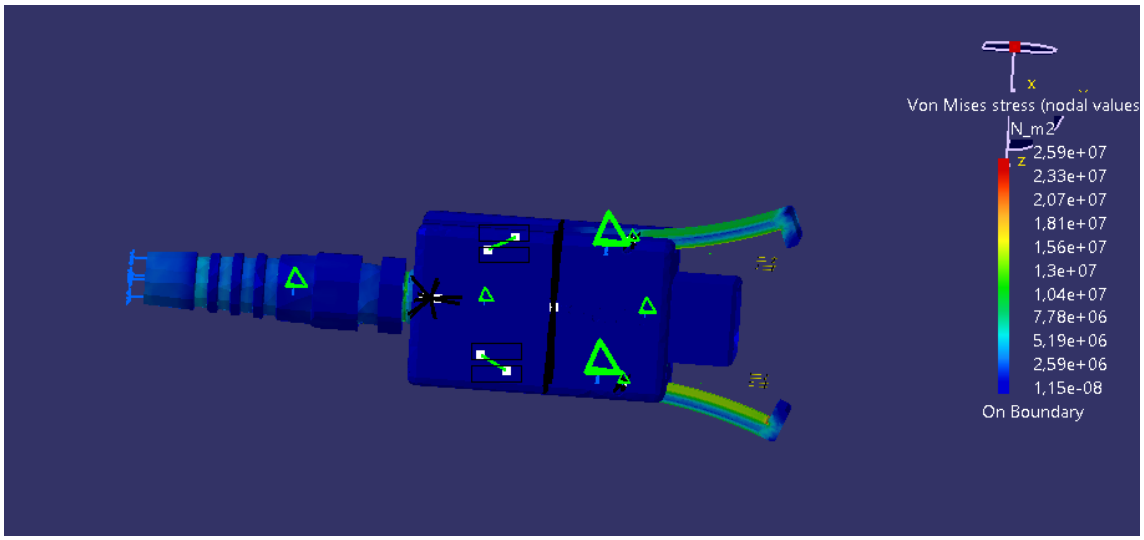

Figure .16: Connector in PETG except the clams.

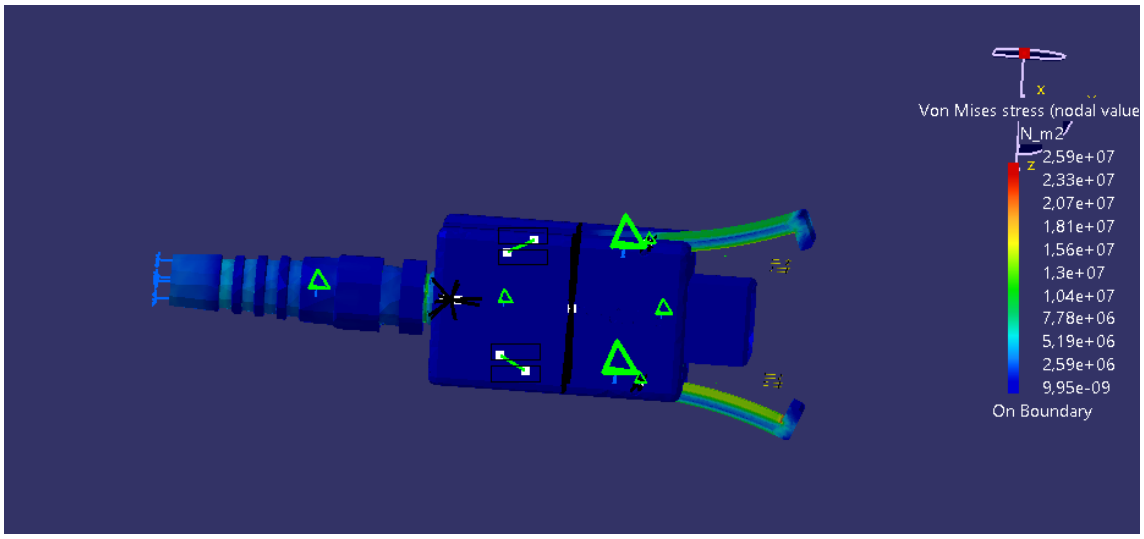

Figure .17: Connector in PETG-CF except the clams.

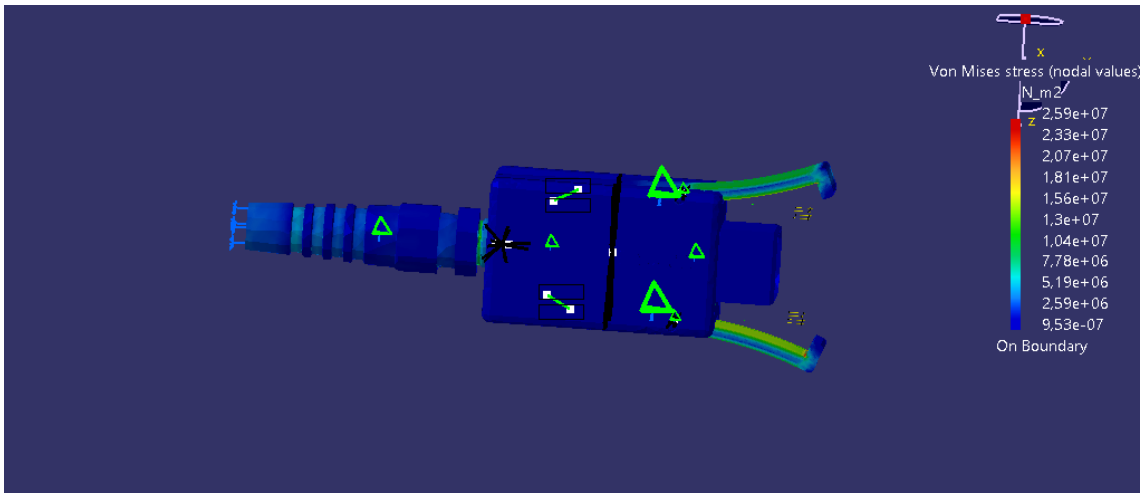

Figure .18: Connector in TPU except the clams.

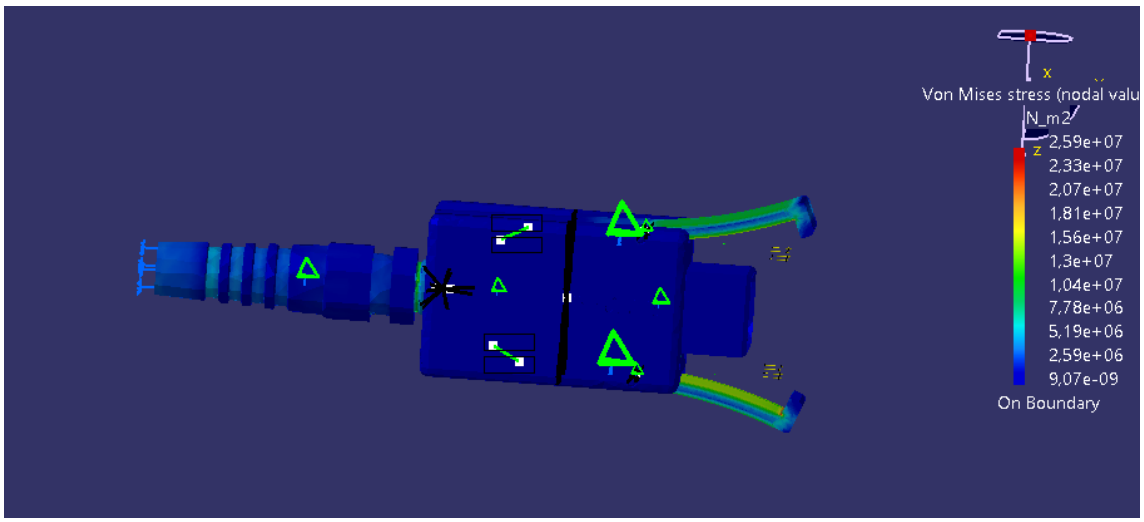

Figure .19: Connector in PATH-CF except the clams.

DEPARTMENT OF SOME SUBJECT OR TECHNOLOGY
CHALMERS UNIVERSITY OF TECHNOLOGY
Gothenburg, Sweden
www.chalmers.se

CHALMERS
UNIVERSITY OF TECHNOLOGY